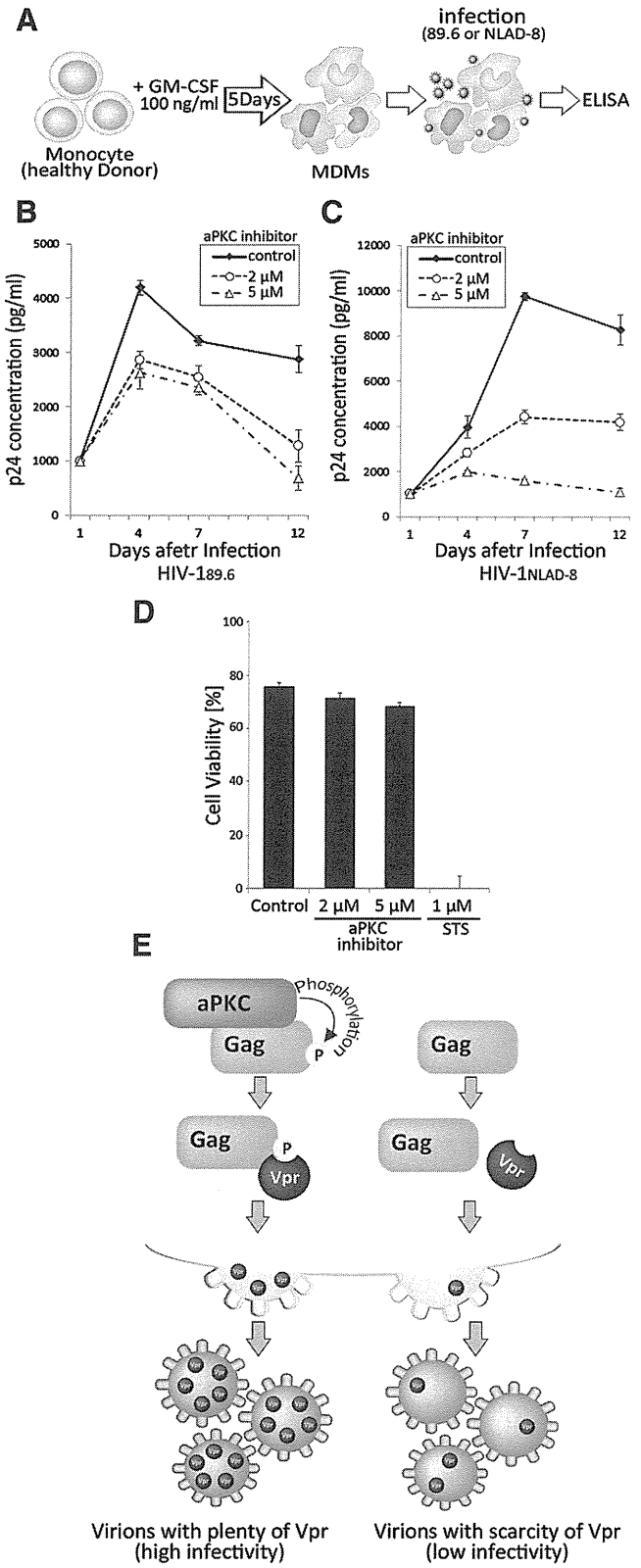

Figure 7 (See legend on next page.)

(See figure on previous page.)
Figure 7 The inhibition of aPKC significantly reduces replication competent HIV-1 infection. (A) Schema of the experimental system using HIV-1 replication competent HIV-$1_{89.6}$ and HIV-1_{NLAD-8}. Monocytes were isolated from buffy coat from healthy blood donors by positive selection on Monocyte Enrichment Cocktail and density gradient centrifugation as described in Methods. MDMs were generated by culturing monocytes with 100 ng/ml granulocyte-macrophage colony-stimulation factor for 5 days before HIV-1 infection. MDMs were infected with 5 ng of p24 from **(B)** HIV-$1_{89.6}$ or **(C)** HIV-1_{NLAD-8} virus and the levels of p24 capsid released into media during viral replication were assayed over a period of 12 days post infection. Data are the mean ± s.e.m. of three independent experiments: $^{**}P < 0.01$, Student's t-test. **(D)** Effects of aPKC inhibitor on viability of MDMs. MDMs cells were treated with aPKC inhibitor (2 or 5 μM) or 1 μM Staurosporine (STS) and analysed for cell viability using trypan blue exclusion at 96 hours. **(E)** Schematic model of our current study. aPKC phosphorylate HIV-1 Gag at Ser487. This phosphorylation promotes the interaction between Gag and Vpr, thereby facilitating viral infectivity in macrophages.

the incorporation of Vpr into virus particles. These specific effects of aPKC-mediated Gag-p6 phosphorylation are consistent with the evidence that the substitution of Gag Ser487 for Ala significantly decreases Vpr incorporation and viral infectivity. On the other hand, inhibition of aPKC in cells may have other additional effects on HIV-1 replication cycle rather than Gag phosphorylation for the Vpr incorporation. To observe the specific effect of aPKC on Gag phosphorylation, we created Gag and Vpr mutants devoid of the effect of aPKC and these mutants were less competent in virus replication. However, aPKC may regulate other cellular function directing HIV replication. Although our current data clearly demonstrate a crucial role of aPKC in Gag Ser487 phosphorylation and interaction Gag-Vpr to Vpr incorporation, further detailed analyses may be necessary to clarify the molecular signature of Gag p6 phosphorylation on multiple stages of the HIV-1 replication cycle.

We show from our current experiments that Gag Ser487 phosphorylation has a significant impact on p6-Vpr binding. Vpr is a non-structural viral protein that is incorporated into virions and possesses several characteristic features and functions that are known to play important roles in HIV-1 replication and disease progression [40]. The presence of a functional Vpr in viral particles is necessary for the efficient translocation of the pre-integration complex (PIC) into the nucleus and subsequent infection of primary monocytes/macrophages and other non-dividing cells [5,6]. Vpr also has a crucial role in viral replication, apoptosis, cell cycle arrest and in the down-regulation of immune activation [37,41-43]. Many Vpr functions are carried out by virion-associated Vpr [44], suggesting that the incorporation of Vpr into virus particles is an important event not only in HIV-1 replication but also in HIV-1 mediated cytopathogenesis.

Several previous reports have indicated that p6 is phosphorylated during HIV-1 infection [2,22]. However, these studies did not undertake any detailed investigation of the biological significance of this phosphorylation event through biochemical or structural analyses. Our current computer-assisted structural modeling and AlphaScreen homogenous proximity assays have revealed that the phosphorylated Gag at Ser487 binds more stably to Vpr whereas there was no significant difference in the interaction of Gag-p6 with Alix, consistent with previous reports [31,32]. The phosphorylation of Ser487 can create another hydrogen bond between Gag-Ser487 and Vpr-Gln44. In consistent with this data a previous study indicated that the site specific deletion of Gln44 resulted in the significant reduction of Vpr incorporation into virions [34]. We also demonstrate that Gag phosphorylation at Ser487 affects Vpr incorporation and this process could be mediated by Gln44 residue of Vpr.

We show in our current study that Gag phosphorylation on Ser487 itself does not affect the binding affinity of Gag with Alix. However, resultant Vpr interaction to Gag may hinder the Alix-Gag interaction at the LYPXnL motif. This may eliminate Alix from nascent VLP and impeded its ability to function in HIV-1 release in PTAP-deficient strains of HIV. On the other hands, Alix also interacts with the nucleocapsid (NC) domain of HIV-1 Gag in addition to binding the LYPXnL motif [45], there by linking Gag to components of ESCRT-III. Therefore, further analysis is needed to fully understand the molecular link between Gag phosphorylation and virus release through the Alix/LYPXnL pathway.

We further explored the physiological significance of Vpr incorporation into virions. Our current results clearly demonstrate that the inhibition of aPKC-mediated Vpr incorporation prominently reduces the viral infectivity in MDMs. These results together indicate that Gag phosphorylation by aPKC plays a crucial role in the HIV-1 infection of macrophages.

aPKC has been demonstrated to be involved in cell polarity and migration in a number of study models [46]. During cell migration, aPKC localizes on the leading edge of the plasma membrane where HIV-1 Gag is also localized in infected cells. It has been reported in an earlier study that aPKC is located at an immunological synapse with potential importance in cell-to-cell viral transfer [47]. It is thus plausible that aPKC may regulate the incorporation of Vpr into virions at the leading edges or the HIV-1 virological synapse in polarized cells [48]. It would be interesting to investigate whether aPKC cooperates with other factors in polarized HIV-1-infected cells in an additional mechanism to its function in Gag phosphorylation.

In the earlier study by Folgueira et al. [49], it was demonstrated that aPKC mediates the NF-κB transcriptional activation required for HIV-1 infection in U937 cells. It is of particular interest that aPKC is a one of the key regulators of HIV-1 infection. Our present findings also provide evidence for the involvement of aPKC in HIV-1 replication by showing that it directly phosphorylates Gag on Ser487, and that this phosphorylation mediates Vpr incorporation into virions. The targeting of aPKC activity is therefore a potential option as a novel therapeutic intervention against HIV-1 infection in combination with existing anti-retroviral treatments.

Conclusions

We have identified aPKC as a host protein kinase that phosphorylates HIV-1 Gag at its Ser487 residue. Computer assisted structural modeling and subsequent biochemical assays revealed that the phosphorylation of Gag Ser487 enhances the association of Gag with Vpr and promotes the resultant incorporation of Vpr into virions. These events facilitate viral infectivity in macrophages. Hence, aPKC inhibition is a potential new therapeutic approach against HIV-1 infection in human macrophages.

Methods

Viral DNA constructs and plasmids

The HIV-1 reporter virus vectors pNL4-3ΔEnv-Luc and pNL4-3ΔEnvΔVpr-Luc were provided by Akifumi Takaori-Kondo (Kyoto University, Kyoto, Japan) [50,51]. The HIV-1 recombinant molecular clone pHIV-$1_{89.6}$ and pHIV-1_{NLAD8} were provided by Akio Adachi (Tokushima University, Tokushima, Japan). The HIV-1 Gag and HIV-1 p6 (pNL4-3) derived-DNA fragment was generated by PCR and inserted into the pEU-E01-GST-MCS vector (Cellfree Sciences, Yokohama, Japan). Using this subcloned plasmid, we generated substitution mutants with PrimSTAR Max (Takara Bio Inc, Shiga, Japan) and the following primers for Ser487A,

5'-TTAACTGCGCTCAGATCACTCTTTGGC-3' and 5'-TCTGAGCGCAGTTAAAGGATACAGTTC-3'. Plasmids expressing HIV-1 Gag-Pol were provided by Jun Komano [52] (National Institute of Infectious Diseases, Tokyo, Japan). Expression vectors encoding aPKCλ wt and aPKCλ kn, a kinase-deficient mutant, have been previously described [53]. C-terminal Flag-tagged p55Gag (codon-optimized) has been previously described [54]. All the DNA experiments were approved by Gene and Recombination Experiment Safety Committee at the Yokohama City University School of Medicine.

Antibodies and other reagents

The anti-p24 (CA) mouse monoclonal antibody (clone Kal-1) was purchased from Dako (Glostrup, Denmark). Anti-Flag (M2) and anti-Vinculin mouse monoclonal antibodies were obtained from Sigma (St. Louis, MO). Anti-PKCι mouse monoclonal antibody was from BD transduction (Franklin Lakes, NJ). Polyclonal rabbit anti-Vpr antibody was obtained from the AIDS research and Reference Reagent Program, National Institute of Allergy and Infectious Diseases (US National Institute of Health, Germantown, MD). The peptide specific antibody against PLT (pS) LRSLFGND (phosphorylated at Ser487 of Gag peptide from 484 to 495) was generated by Scrum Inc (Tokyo, Japan). The myristoylated (myr) PKC ζ peptide inhibitor myr-PKCζ (N-myr-Ser-Ile-Tyr-Arg-Arg-Gly-Ala-Arg-Arg-Trp-Arg-Lys-Leu-OH) and myr-PKC α and β (N-myr-Phe-Ala-Arg-Lys-Gly-Ala-Leu-Arg-Gln-NH_2) were purchased from Merck (Darmstadt, Germany). Akt inhibitor was obtained from Calbiochem (Darmstadt, Germany), and the PI3K inhibitor Wortmannin was obtained from Merck. The Cdk inhibitor roscovitine was purchased from Promega (Madison, WI). All inhibitors were dissolved in DMSO and stocks were aliquoted and stored at −60°C until use. The final concentration of each inhibitor used is indicated in the figure legends.

Cells and viruses

Monocytes were isolated from buffy coat from healthy blood donors by positive selection on Monocyte Enrichment Cocktail (Stemcell, Tukwila, WA) and Lymphoprep (Stemcell) density gradient centrifugation with SepMate-50 (Stemcell). MDMs were generated by culturing monocytes with 100 ng/ml granulocyte-macrophage colony-stimulation factor for 5 days. 293T and HeLa cells were cultured in DMEM (Gibco-BRL, Rockville, MD) supplemented with 10% (V/V) fetal bovine serum (FBS) (Gibco-BRL). HIV-$1_{89.6}$ and HIV-1_{NLAD-8} strains were produced in 293T cells. Vesicular stomatitis virus G glycoprotein (VSV-G)-pseudotyped viruses were produced in 293T cells cotransfected with reporter virus plasmid and VSV-G using the calcium-phosphate method. The culture supernatants were collected and subjected to quantification of HIV-1 particle yields by p24CA antigen capture enzyme-linked immunosorbent assay (ELISA) (Zepto Metrix, Buffalo, NY). Monocyte isolation and treatment were approved by the Ethics Committee at the Yokohama City University School of Medicine.

In vitro protein production

A total of 287 cDNAs encoding human protein kinases were constructed as described previously [23]. The protein production method has also been described previously [55-57]. Briefly, DNA templates containing a biotin-ligating sequence were amplified by split-PCR using cDNAs and corresponding primers, and then used with the GenDecoder protein production system (Cell Free Science, Ehime, Japan). For HIV-1 Gag protein synthesis, *Gag* genes derived from the pNL4-3 proviral plasmid [58] were

generated by split-PCR, and used as template with a Wheat Germ Expression kit (Cell Free Science) in accordance with the manufacturer's instructions.

Alphascreen-based protein-protein interaction assays

AlphaScreen assays were performed as described previously [23]. All recombinant proteins used here was synthesized using a wheat germ based cell-free system as described above. For each protein kinase, 1 μl of crude recombinant biotinylated construct from the human kinase library was incubated with 1 μl of crude GST-Gag or GST-DHFR in 10 μl of kinase assay buffer (100 mM Tris–HCl pH8.0, 10 mM $MgCl_2$, 0.1% Tween20, 0.1% BSA) at 37°C for 1 h in one well of a 384-well Optiplate (Perkin Elmer, Foster City, CA. In accordance with the AlphaScreen IgG (protein A) detection kit (Perkin Elmer) instruction manual, 15 μl of detection mixture containing 100 mM Tris–HCl pH 8.0, 0.01% Tween-20, 1 mg/ml BSA, 5 μg/ml Anti-FLAG antibody (GE healthcare, Buckinghamshire, UK), 5 ng streptavidin-coated donor beads and 5 ng anti-IgG (protein A) acceptor beads were added to each well followed by incubation at 26°C for 1 h. AlphaScreen signals from the mixture were detected using an EnVision device (PerkinElmer) with the AlphaScreen signal detection program.

In vitro kinase assays

Biotinylated GST-Gag proteins were synthesized in wheat germ cell-free extracts as described above. The synthesized GST-Gag proteins were then purified using streptavidin conjugated magnet beads (Promega). The purified proteins on the beads were then incubated with recombinant aPKCiota (Cell Signaling Technology) in a 50 μl reaction mixture containing 20 mM Tris–HCl pH 7.5, 1 mM EDTA, 1 mM dithiothreitol, 150 mM NaCl, 5 mM $MgCl_2$, 0.05% Tween-20, 100 μM ATP and 2 μCi [γ-^{32}P] ATP. The reaction mixture was then incubated for 1 h at 37°C, and the products were subjected to electrophoresis on 10% SDS polyacrylamide gels and were detected with an image guider (BAS2500; Fujifilm, Tokyo, Japan).

Western blotting

Cells were harvested at the indicated post-treatment time points with doxycycline, washed with phosphate-buffer saline (PBS), and treated with lysis buffer (0.02% sodium dodecyl sulfate [SDS], 0.5% Triton X-100, 300 mM NaCl, 20 mM Tris–HCl [pH 7.6], 1 mM EDTA, 1 mM dithiothreitol) for 20 min on ice. Multiple protease inhibitors, 200 μM sodium vanadate and 20 mM sodium fluoride were then added to the buffer. The samples were centrifuged at 18,000 g for 10 min at 4°C, and clarified cell extracts were assayed for protein concentration using a Bio-Rad kit. Equal amounts of proteins (20 ~ 50 μg) were resolved by SDS-10% polyacrylamide (acrylamide, 29.2; bisacrylamide, 0.8) gel electrophoresis (SDS-PAGE) in running buffer (250 mM glycine, 25 mM Tris, 0.1% SDS). The separated proteins were transferred to polyvinylidene difluoride membrane. The membranes were washed with blotting buffer (TBS containing 0.1% Tween 20) and blocked in 10% low-fat powdered milk in blotting buffer for 1 h at room temperature. Primary antibodies were added at appropriate dilutions in 3% bovine serum albumin in blotting buffer and rocked overnight at 4°C. The membranes were then further washed in blotting buffer and incubated with a horseradish peroxidase-conjugated secondary antibody at room temperature for 1 h. Target proteins were detected with an enhanced chemiluminescence detection system (GE Healthcare). Images were processed using Fluor Chem FC2 (Alpha Innotech Corp. Tokyo, Japan) with a cooled charge-coupled device (CCD) camera and assembled using Adobe Photoshop CS5 Extended.

Identification of phosphorylation sites on HIV-1 gag by mass spectrometry

Samples were separated by SDS-PAGE (12.5%) and the gel was stained with Coomassie brilliant blue (CBB). Gag was excised from the stained gel and digested with trypsin in 50 mM NH_4HCO_3 (pH 8.0) for 12 h at 37°C. Phosphopeptides were enriched using Titansphere® Phos-TiO Kit (GLsciences, Tokyo, Japan), in accordance with the manufacturer's instructions. The enriched phosphopeptides were then analyzed by MALDI-TOF/TOF-MS (4800 proteomics analyzer, AB SCIEX, Foster City, CA). The resulting raw MS spectrum was processed using the 4000 Series Explorer Software (AB SCIEX, Framingham, MA) to generate Mascot generic format. The obtained MS and MS/MS data were then searched against the SwissProt database (January, 2013; 538849 sequences) using Mascot version 2.4.1 software (Matrix Science, London, UK), to identify proteins and protein modification. The search parameters were as follows: trypsin digestion with two missed cleavages permitted, variable modifications (oxidation of Met and phosphorylation of Ser, Thr, and Tyr), peptide mass tolerance for MS data ±0.15 Da, and fragment mass tolerance ±0.3 Da. Phosphopeptides were determined primarily using the Mascot program and were confirmed manually through raw MS/MS sequence data checking for the neutral loss of the phosphate group (−98).

Analysis of structural data and structural model construction

The 3D structure of Alix with wild-type Gag-p6 was predicted by homology modeling using Molecular Operating Environment (MOE) (Chemical Computing Group, Canada). X-ray crystal structure of Gag-p6-Alix (Protein Data Bank [PDB] code: 2R02) was used as

template structure. Energy calculation was achieved with AMBER ff99 force field and the GB/VI implicit solvent energy function [59]. Next, on the basis of the predicted structural model of Alix with wild-type Gag-p6, 3D structures of Alix with Gag-p6S487A and phosphorylated Gag-p6-Ser487 were constructed using Molecular Builder in MOE.

3D structures of Vpr with wild-type Gag-p6, Gag-p6Ser487A, and phosphorylated Gag-p6-Ser487 were also predicted by docking simulations with ASEdock module in MOE, because of no complex structure of Gag-p6-Vpr. The complex structure was estimated with a nuclear magnetic resonance (NMR) structure of Vpr (PDB code: 1M8L [60]) and a NMR structure around helix II domain of Gag-p6 (Gag Y483 to S494) (PDB code: 2C55). Substitution and phosphorylation at Gag S487 were achieved with the Molecular Builder. Energy calculations in the docking simulations were achieved with the same force field as that for Gag-p6-Alix.

Finally, all of the constructed complex structures were thermodynamically optimized with energy minimization, to remove unfavorable steric contacts.

Bimolecular fluorescence complementation assay (BiFC)

To detect interaction of Gag with Vpr, we used the BiFC technique. Briefly, two fragments of Kusabira-Green (KG) fluorescent protein are brought together by the interaction of two proteins fused to these fragments, thus allowing specific detection of interaction in living cells (Amalgaam). Vpr or Vpr Q44E were cloned into phmKGN-MN and Gag or GagSer487A into phmKGC-MC. 293T cells were cotransfected with 0.7 μg of the Vpr construct and 0.5 μg of the Gag construct. Two days post transfection, cells were harvested and then subjected to the flow cytometry for measuring BiFC signal as reported previously [34].

Immunoprecipitation

Cells were lysed in Lysis buffer containing 50 mM Tris–HCl (pH 8.0), 150 mM NaCl, 1 mM EDTA, 1 mM DTT with Complete protease inhibitor cocktail (Roche Molecular Biochemicals, Indianapolis, IN) and PhosSTOP phosphatase inhibitor cocktail (Roche Molecular Biochemicals). Lysate were cleared by centrifugation at 12,000 × g for 15 min, followed by pull down using with anti-Flag M2 affinity Gel (Sigma). Samples were separated by SDS-PAGE and analysed by Western blot analyses.

Single-cycle virus release assays

For infection-based assays, cells were infected with VSV-G-pseudotyped HIV-1 at an moi (multiplicity of infection) of 0.01 or 0.2 for eight hours and cultured for two days. In experiments using kinase inhibitors, cells were treated with each inhibitor at 12 h before virus infection. Virus-containing supernatants were harvested and filtered to remove cell debris, and viral p24 antigens were measured using an ELISA kit (Zepto Metrix). The cell lysates were prepared using HBST buffer (10 mM HEPES, pH 7.4, 150 mM NaCl, 0.5% Triton X-100) containing a protease inhibitor cocktail (Roche). Immunoblotting assays and the antibodies used have been described previously [61]. The culture supernatants and cell lysates were subjected to p24 ELISA or immunoblotting assays, as described above.

HIV-1 production assay

Primary human macrophages were infected with HIV-$1_{89.6}$ or HIV-$1_{NLAD\text{-}8}$ virus. Two days post-infection, these cells were washed with PBS to eliminate the presence of virus. After washing, the cells were cultured either in media alone or media containing aPKC inhibitor. Infected macrophages were cultured for 12 days, during which time viral supernatants were collected and fresh media with inhibitors was also added every three days. The p24 levels contained in each viral supernatant sample was monitored using p24 ELISA (Zepto Metrix) in accordance with the manufacturer's protocol.

Competing interests

The authors declare that they have no competing interests.

Authors' contributions

AK, ST, HO, KM, AO and AI performed experiments. AK, ST, TS, SM, HK, WS, HS, HH, SO, NY and AR participated in the design of the study, the analysis of the data. AK and AR wrote the manuscript. All authors read and approved the final manuscript.

Acknowledgements

We gratefully acknowledge Akifumi Takaori-Kondo (Kyoto University) for providing the reporter virus vectors pNL4-3ΔEnv-Luc and pNL4-3ΔEnvΔVpr-Luc, Akio Adachi (Tokushima University) for providing Flag-Vpr expression vector, HIV-1 molecular clone vectors for HIV-$1_{89.6}$, and HIV-$1_{NLAD\text{-}8}$, Akinori Takaoka (Hokkaido University) for kindly providing a material and discussion, Andrés Finzi (Université de Montréal) for helpful discussion, Noriko Ikawa (Yokohama City University) for technical assistance. HIV-1 Vpr (1–50) antiserum was obtained through the AIDS Research and Reference Reagent Program, Division of AIDS, NIAID, NIH from Jeffrey Kopp.

Author details

[1]Department of Microbiology, Yokohama City University School of Medicine, Yokohama, Kanagawa, Japan. [2]Venture Business Laboratory, Ehime University, Matsuyama, Ehime, Japan. [3]Proteo-Science Center, Ehime University, Matsuyama, Ehime, Japan. [4]Clinical Research Center, National Hospital Organization Nagoya Medical Center, Nagoya, Aichi, Japan. [5]Pathogen Genomics Center, National Institute of Infectious Diseases, Musashi Murayama, Tokyo, Japan. [6]Supramolecular Biology, International Graduate School of Arts and Sciences, Yokohama City University, Yokohama, Kanagawa, Japan. [7]Infectious Disease Surveillance Center, National Institute of Infectious Diseases, Musashi Murayama, Tokyo, Japan. [8]Department of Molecular Biology, Yokohama City University School of Medicine, Yokohama, Kanagawa, Japan. [9]Department of Microbiology, National University of Singapore, Singapore, Singapore.

Received: 25 July 2013 Accepted: 12 January 2014
Published: 22 January 2014

References

1. Barnitz RA, Wan F, Tripuraneni V, Bolton DL, Lenardo MJ: **Protein kinase A phosphorylation activates Vpr-induced cell cycle arrest during human immunodeficiency virus type 1 infection.** *J Virol* 2010, **84**(13):6410–6424.
2. Hemonnot B, Cartier C, Gay B, Rebuffat S, Bardy M, Devaux C, Boyer V, Briant L: **The host cell MAP kinase ERK-2 regulates viral assembly and release by phosphorylating the p6gag protein of HIV-1.** *J Biol Chem* 2004, **279**(31):32426–32434.
3. Ammosova T, Berro R, Jerebtsova M, Jackson A, Charles S, Klase Z, Southerland W, Gordeuk VR, Kashanchi F, Nekhai S: **Phosphorylation of HIV-1 Tat by CDK2 in HIV-1 transcription.** *Retrovirology* 2006, **3**:78.
4. Adamson CS, Freed EO: **Human immunodeficiency virus type 1 assembly, release, and maturation.** *Adv Pharmacol* 2007, **55**:347–387.
5. Subbramanian RA, Kessous-Elbaz A, Lodge R, Forget J, Yao XJ, Bergeron D, Cohen EA: **Human immunodeficiency virus type 1 Vpr is a positive regulator of viral transcription and infectivity in primary human macrophages.** *J Exp Med* 1998, **187**(7):1103–1111.
6. Connor RI, Chen BK, Choe S, Landau NR: **Vpr is required for efficient replication of human immunodeficiency virus type-1 in mononuclear phagocytes.** *Virology* 1995, **206**(2):935–944.
7. Levy DN, Refaeli Y, Weiner DB: **Extracellular Vpr protein increases cellular permissiveness to human immunodeficiency virus replication and reactivates virus from latency.** *J Virol* 1995, **69**(2):1243–1252.
8. de Marco A, Muller B, Glass B, Riches JD, Krausslich HG, Briggs JA: **Structural analysis of HIV-1 maturation using cryo-electron tomography.** *PLoS Pathog* 2010, **6**(11):e1001215.
9. Morita E, Sundquist WI: **Retrovirus budding.** *Annu Rev Cell Dev Biol* 2004, **20**:395–425.
10. Demirov DG, Orenstein JM, Freed EO: **The late domain of human immunodeficiency virus type 1 p6 promotes virus release in a cell type-dependent manner.** *J virology* 2002, **76**(1):105–117.
11. Garrus JE, von Schwedler UK, Pornillos OW, Morham SG, Zavitz KH, Wang HE, Wettstein DA, Stray KM, Cote M, Rich RL, *et al*: **Tsg101 and the vacuolar protein sorting pathway are essential for HIV-1 budding.** *Cell* 2001, **107**(1):55–65.
12. Strack B, Calistri A, Craig S, Popova E, Gottlinger HG: **AIP1/ALIX is a binding partner for HIV-1 p6 and EIAV p9 functioning in virus budding.** *Cell* 2003, **114**(6):689–699.
13. von Schwedler UK, Stuchell M, Muller B, Ward DM, Chung HY, Morita E, Wang HE, Davis T, He GP, Cimbora DM, *et al*: **The protein network of HIV budding.** *Cell* 2003, **114**(6):701–713.
14. Fujii K, Hurley JH, Freed EO: **Beyond Tsg101: the role of Alix in 'ESCRTing' HIV-1.** *Nat rev Microbiol* 2007, **5**(12):912–916.
15. Bieniasz PD: **Late budding domains and host proteins in enveloped virus release.** *Virology* 2006, **344**(1):55–63.
16. Morita E, Sandrin V, McCullough J, Katsuyama A, Baci Hamilton I, Sundquist WI: **ESCRT-III protein requirements for HIV-1 budding.** *Cell Host Microbe* 2011, **9**(3):235–242.
17. Fujii K, Munshi UM, Ablan SD, Demirov DG, Soheilian F, Nagashima K, Stephen AG, Fisher RJ, Freed EO: **Functional role of Alix in HIV-1 replication.** *Virology* 2009, **391**(2):284–292.
18. Salgado GF, Marquant R, Vogel A, Alves ID, Feller SE, Morellet N, Bouaziz S: **Structural studies of HIV-1 Gag p6ct and its interaction with Vpr determined by solution nuclear magnetic resonance.** *Biochemistry* 2009, **48**(11):2355–2367.
19. Paxton W, Connor RI, Landau NR: **Incorporation of Vpr into human immunodeficiency virus type 1 virions: requirement for the p6 region of gag and mutational analysis.** *J Virol* 1993, **67**(12):7229–7237.
20. Belzile JP, Abrahamyan LG, Gerard FC, Rougeau N, Cohen EA: **Formation of mobile chromatin-associated nuclear foci containing HIV-1 Vpr and VPRBP is critical for the induction of G2 cell cycle arrest.** *PLoS Pathog* 2010, **6**(9):e1001080.
21. Solbak SM, Reksten TR, Roder R, Wray V, Horvli O, Raae AJ, Henklein P, Fossen T: **HIV-1 p6-Another viral interaction partner to the host cellular protein cyclophilin A.** *Biochim Biophys Acta* 2012, **1824**(4):667–678.
22. Muller B, Patschinsky T, Krausslich HG: **The late-domain-containing protein p6 is the predominant phosphoprotein of human immunodeficiency virus type 1 particles.** *J Virol* 2002, **76**(3):1015–1024.
23. Tadokoro D, Takahama S, Shimizu K, Hayashi S, Endo Y, Sawasaki T: **Characterization of a caspase-3-substrate kinome using an N- and C-terminally tagged protein kinase library produced by a cell-free system.** *Cell Death Dis* 2010, **1**:e89.
24. Burnette B, Yu G, Felsted RL: **Phosphorylation of HIV-1 gag proteins by protein kinase C.** *J Biol Chem* 1993, **268**(12):8698–8703.
25. Cartier C, Sivard P, Tranchat C, Decimo D, Desgranges C, Boyer V: **Identification of three major phosphorylation sites within HIV-1 capsid. Role of phosphorylation during the early steps of infection.** *J Biol Chem* 1999, **274**(27):19434–19440.
26. Newton AC: **Regulation of protein kinase C.** *Curr Opin Cell Biol* 1997, **9**(2):161–167.
27. Guendel I, Agbottah ET, Kehn-Hall K, Kashanchi F: **Inhibition of human immunodeficiency virus type-1 by cdk inhibitors.** *AIDS Res Ther* 2010, **7**(1):7.
28. Deregibus MC, Cantaluppi V, Doublier S, Brizzi MF, Deambrosis I, Albini A, Camussi G: **HIV-1-Tat protein activates phosphatidylinositol 3-kinase/AKT-dependent survival pathways in Kaposi's sarcoma cells.** *J Biol Chem* 2002, **277**(28):25195–25202.
29. Chugh P, Fan S, Planelles V, Maggirwar SB, Dewhurst S, Kim B: **Infection of human immunodeficiency virus and intracellular viral Tat protein exert a pro-survival effect in a human microglial cell line.** *J Mol Biol* 2007, **366**(1):67–81.
30. Yu G, Shen FS, Sturch S, Aquino A, Glazer RI, Felsted RL: **Regulation of HIV-1 gag protein subcellular targeting by protein kinase C.** *J Biol Chem* 1995, **270**(9):4792–4796.
31. Fisher RD, Chung HY, Zhai Q, Robinson H, Sundquist WI, Hill CP: **Structural and biochemical studies of ALIX/AIP1 and its role in retrovirus budding.** *Cell* 2007, **128**(5):841–852.
32. Lazert C, Chazal N, Briant L, Gerlier D, Cortay JC: **Refined study of the interaction between HIV-1 p6 late domain and ALIX.** *Retrovirology* 2008, **5**:39.
33. Votteler J, Neumann L, Hahn S, Hahn F, Rauch P, Schmidt K, Studtrucker N, Solbak SM, Fossen T, Henklein P, *et al*: **Highly conserved serine residue 40 in HIV-1 p6 regulates capsid processing and virus core assembly.** *Retrovirology* 2011, **8**:11.
34. Venkatachari NJ, Walker LA, Tastan O, Le T, Dempsey TM, Li Y, Yanamala N, Srinivasan A, Klein-Seetharaman J, Montelaro RC, *et al*: **Human immunodeficiency virus type 1 Vpr: oligomerization is an essential feature for its incorporation into virus particles.** *Virology J* 2010, **7**:119.
35. Balliet JW, Kolson DL, Eiger G, Kim FM, McGann KA, Srinivasan A, Collman R: **Distinct effects in primary macrophages and lymphocytes of the human immunodeficiency virus type 1 accessory genes vpr, vpu, and nef: mutational analysis of a primary HIV-1 isolate.** *Virology* 1994, **200**(2):623–631.
36. Heinzinger NK, Bukinsky MI, Haggerty SA, Ragland AM, Kewalramani V, Lee MA, Gendelman HE, Ratner L, Stevenson M, Emerman M: **The Vpr protein of human immunodeficiency virus type 1 influences nuclear localization of viral nucleic acids in nondividing host cells.** *Proc Natl Acad Sci USA* 1994, **91**(15):7311–7315.
37. Vodicka MA, Koepp DM, Silver PA, Emerman M: **HIV-1 Vpr interacts with the nuclear transport pathway to promote macrophage infection.** *Genes Dev* 1998, **12**(2):175–185.
38. Solbak SM, Reksten TR, Hahn F, Wray V, Henklein P, Halskau O, Schubert U, Fossen T: **HIV-1 p6 - a structured to flexible multifunctional membrane-interacting protein.** *Biochim Biophys Acta* 2013, **1828**(2):816–823.
39. Radestock B, Morales I, Rahman SA, Radau S, Glass B, Zahedi RP, Muller B, Krausslich HG: **Comprehensive mutational analysis reveals p6Gag phosphorylation to be dispensable for HIV-1 morphogenesis and replication.** *J Virol* 2013, **87**(2):724–734.
40. Lai M, Chen J: **The role of Vpr in HIV-1 disease progression is independent of its G2 arrest induction function.** *Cell Cycle* 2006, **5**(19):2275–2280.
41. Sawaya BE, Khalili K, Gordon J, Taube R, Amini S: **Cooperative interaction between HIV-1 regulatory proteins Tat and Vpr modulates transcription of the viral genome.** *J Biol Chem* 2000, **275**(45):35209–35214.
42. Chang F, Re F, Sebastian S, Sazer S, Luban J: **HIV-1 Vpr induces defects in mitosis, cytokinesis, nuclear structure, and centrosomes.** *Mol Biol Cell* 2004, **15**(4):1793–1801.
43. Ramanathan MP, Curley E 3rd, Su M, Chambers JA, Weiner DB: **Carboxyl terminus of hVIP/mov34 is critical for HIV-1-Vpr interaction and glucocorticoid-mediated signaling.** *J Biol Chem* 2002, **277**(49):47854–47860.
44. Romani B, Engelbrecht S: **Human immunodeficiency virus type 1 Vpr: functions and molecular interactions.** *J Gen Virol* 2009, **90**(Pt 8):1795–1805.

45. Dussupt V, Javid MP, Abou-Jaoude G, Jadwin JA, de La Cruz J, Nagashima K, Bouamr F: **The nucleocapsid region of HIV-1 Gag cooperates with the PTAP and LYPXnL late domains to recruit the cellular machinery necessary for viral budding.** *PLoS Pathog* 2009, **5**(3):e1000339.
46. Rosse C, Linch M, Kermorgant S, Cameron AJ, Boeckeler K, Parker PJ: **PKC and the control of localized signal dynamics.** *Nat Rev Mol Cell Biol* 2010, **11**(2):103–112.
47. Yuseff MI, Reversat A, Lankar D, Diaz J, Fanget I, Pierobon P, Randrian V, Larochette N, Vascotto F, Desdouets C, *et al*: **Polarized secretion of lysosomes at the B cell synapse couples antigen extraction to processing and presentation.** *Immunity* 2011, **35**(3):361–374.
48. Gousset K, Ablan SD, Coren LV, Ono A, Soheilian F, Nagashima K, Ott DE, Freed EO: **Real-time visualization of HIV-1 GAG trafficking in infected macrophages.** *PLoS Pathog* 2008, **4**(3):e1000015.
49. Folgueira L, McElhinny JA, Bren GD, MacMorran WS, Diaz-Meco MT, Moscat J, Paya CV: **Protein kinase C-zeta mediates NF-kappa B activation in human immunodeficiency virus-infected monocytes.** *J Virol* 1996, **70**(1):223–231.
50. Kobayashi M, Takaori-Kondo A, Miyauchi Y, Iwai K, Uchiyama T: **Ubiquitination of APOBEC3G by an HIV-1 Vif-Cullin5-Elongin B-Elongin C complex is essential for Vif function.** *J Biol Chem* 2005, **280**(19):18573–18578.
51. Izumi T, Io K, Matsui M, Shirakawa K, Shinohara M, Nagai Y, Kawahara M, Kobayashi M, Kondoh H, Misawa N, *et al*: **HIV-1 viral infectivity factor interacts with TP53 to induce G2 cell cycle arrest and positively regulate viral replication.** *Proc Natl Acad Sci USA* 2010, **107**(48):20798–20803.
52. Urano E, Aoki T, Futahashi Y, Murakami T, Morikawa Y, Yamamoto N, Komano J: **Substitution of the myristoylation signal of human immunodeficiency virus type 1 Pr55Gag with the phospholipase C-delta1 pleckstrin homology domain results in infectious pseudovirion production.** *J Gen Virol* 2008, **89**(Pt 12):3144–3149.
53. Yamanaka T, Horikoshi Y, Suzuki A, Sugiyama Y, Kitamura K, Maniwa R, Nagai Y, Yamashita A, Hirose T, Ishikawa H, *et al*: **PAR-6 regulates aPKC activity in a novel way and mediates cell-cell contact-induced formation of the epithelial junctional complex.** *Genes Cells* 2001, **6**(8):721–731.
54. Ryo A, Tsurutani N, Ohba K, Kimura R, Komano J, Nishi M, Soeda H, Hattori S, Perrem K, Yamamoto M, *et al*: **SOCS1 is an inducible host factor during HIV-1 infection and regulates the intracellular trafficking and stability of HIV-1 Gag.** *Proc Natl Acad Sci USA* 2008, **105**(1):294–299.
55. Sawasaki T, Ogasawara T, Morishita R, Endo Y: **A cell-free protein synthesis system for high-throughput proteomics.** *Proc Natl Acad Sci USA* 2002, **99**(23):14652–14657.
56. Sawasaki T, Morishita R, Gouda MD, Endo Y: **Methods for high-throughput materialization of genetic information based on wheat germ cell-free expression system.** *Methods Mol Biol* 2007, **375**:95–106.
57. Takai K, Sawasaki T, Endo Y: **Practical cell-free protein synthesis system using purified wheat embryos.** *Nat Protoc* 2010, **5**(2):227–238.
58. Adachi A, Gendelman HE, Koenig S, Folks T, Willey R, Rabson A, Martin MA: **Production of acquired immunodeficiency syndrome-associated retrovirus in human and nonhuman cells transfected with an infectious molecular clone.** *J Virol* 1986, **59**(2):284–291.
59. Labute P: **The generalized Born/volume integral implicit solvent model: estimation of the free energy of hydration using London dispersion instead of atomic surface area.** *J Comput Chem* 2008, **29**(10):1693–1698.
60. Morellet N, Bouaziz S, Petitjean P, Roques BP: **NMR structure of the HIV-1 regulatory protein VPR.** *J Mol Biol* 2003, **327**(1):215–227.
61. Miyakawa K, Ryo A, Murakami T, Ohba K, Yamaoka S, Fukuda M, Guatelli J, Yamamoto N: **BCA2/Rabring7 promotes tetherin-dependent HIV-1 restriction.** *PLoS Pathog* 2009, **5**(12):e1000700.

doi:10.1186/1742-4690-11-9
Cite this article as: Kudoh *et al.*: The phosphorylation of HIV-1 Gag by atypical protein kinase C facilitates viral infectivity by promoting Vpr incorporation into virions. *Retrovirology* 2014 11:9.

Journal of General Virology (2013), **94**, 933–943 DOI 10.1099/vir.0.047167-0

Impact of antiretroviral pressure on selection of primary human immunodeficiency virus type 1 envelope sequences *in vitro*

Shigeyoshi Harada,[1,2] Kazuhisa Yoshimura,[1,2] Aki Yamaguchi,[1] Samatchaya Boonchawalit,[1,2] Keisuke Yusa[3] and Shuzo Matsushita[1]

Correspondence
Kazuhisa Yoshimura
ykazu@nih.go.jp

[1]Center for AIDS Research, Kumamoto University, 2-2-1 Honjo, Chuo-ku, Kumamoto 860-0811, Japan

[2]AIDS Research Center, National Institute of Infectious Diseases, 1-23-1 Toyama, Shinjuku-ku, Tokyo 162-8640, Japan

[3]Division of Biological Chemistry and Biologicals, National Institute of Health Sciences, 1-18-1 Kami-youga, Setagaya-ku, Tokyo 158-8501, Japan

Received 15 August 2012
Accepted 20 December 2012

The initiation of drug therapy results in a reduction in the human immunodeficiency virus type 1 (HIV-1) population, which represents a potential genetic bottleneck. The effect of this drug-induced genetic bottleneck on the population dynamics of the envelope (Env) regions has been addressed in several *in vivo* studies. However, it is difficult to investigate the effect on the *env* gene of the genetic bottleneck induced not only by entry inhibitors but also by non-entry inhibitors, particularly *in vivo*. Therefore, this study used an *in vitro* selection system using unique bulk primary isolates established in the laboratory to observe the effects of the antiretroviral drug-induced bottleneck on the integrase and *env* genes. Env diversity was decreased significantly in one primary isolate [KP-1, harbouring both CXCR4 (X4)- and CCR5 (R5)-tropic variants] when passaged in the presence or absence of raltegravir (RAL) during *in vitro* selection. Furthermore, the RAL-selected KP-1 variant had a completely different Env sequence from that in the passage control (particularly evident in the gp120, V1/V2 and V4-loop regions), and a different number of potential *N*-glycosylation sites. A similar pattern was also observed in other primary isolates when using different classes of drugs. This is the first study to explore the influence of anti-HIV drugs on bottlenecks in bulk primary HIV isolates with highly diverse Env sequences using *in vitro* selection.

INTRODUCTION

Human immunodeficiency virus type 1 (HIV-1) shows a high degree of genetic diversity owing to its high rates of replication and recombination and the high mutation rate of the HIV-1 reverse transcriptase (Nájera *et al.*, 2002). Even in a single infected individual, the virus can best be described as a population of distinct, but closely related, genetic variants or 'quasi-species' (Eigen, 1993; Nijhuis *et al.*, 1998). The quasi-species behaviour of viruses is recognized as a key element in our understanding and modelling of viral evolution and disease control (Vignuzzi *et al.*, 2006).

Combination antiretroviral (ARV) therapy results in a contraction of the viral population, which represents a potential genetic bottleneck (Charpentier *et al.*, 2006; Delwart *et al.*, 1998; Ibáñez *et al.*, 2000; Kitrinos *et al.*, 2005; Nijhuis *et al.*, 1998; Nora *et al.*, 2007; Sheehy *et al.*, 1996; Zhang *et al.*, 1994). Whilst this bottleneck has a direct effect on the region that is being targeted by the drugs (e.g. protease or reverse transcriptase), it also affects other regions of the viral genome. Indeed, the effect of the drug-induced genetic bottleneck on the population dynamics of the envelope (Env) regions has been addressed in several *in vivo* studies (Charpentier *et al.*, 2006; Delwart *et al.*, 1998; Ibáñez *et al.*, 2000; Kitrinos *et al.*, 2005; Nijhuis *et al.*, 1998; Nora *et al.*, 2007; Sheehy *et al.*, 1996; Zhang *et al.*, 1994).

Virus bottleneck evolution of the HIV-1 *env* gene might be important when choosing the optimal drugs to treat a particular patient. Indeed, a CCR5 antagonist (maraviroc, MVC) and a fusion inhibitor (enfuvirtide, T-20) have now

The GenBank/EMBL/DDBJ accession numbers for the *env* sequences of HIV-1 KP-1, KP-2 and KP-4, are AB640872–AB640881, AB641341–AB641351 and AB641335–AB641340, respectively.

Two supplementary figures are available with the online version of this paper.

been approved for use as HIV-1 entry inhibitors. Analysing the dynamics of drug-induced genetic bottlenecks and studying drug-resistant mutation profiles in response to HIV-1-specific ARV drugs are both important if we are to understand fully HIV-1 drug resistance and pathogenesis.

The aim of the present study was to understand better the effect of *in vivo* drug-induced genetic bottlenecks. *In vitro* selection of different primary HIV-1 isolates was performed using the recently approved HIV integrase inhibitor raltegravir (RAL) (Steigbigel *et al.*, 2008). Two R5-, one X4-, one dual- and one mixed R5/X4-tropic isolates were passaged through a RAL-induced genetic bottleneck. We also performed *in vitro* selection of the R5/X4 isolate using lamivudine (3TC), saquinavir (SQV) and MVC, and compared the results with those from the RAL-selected isolate.

RESULTS

Genotypic profiles of the HIV-1 primary isolates

Four genetically heterogeneous HIV-1 primary isolates (KP-1–4) from Japanese drug-naïve patients were used to assess the extent to which RAL affected the selection of bulk primary viruses *in vitro*. A laboratory isolate, strain 89.6, was also used in the study (rather than a molecular clone) to allow escape mutants to be selected from each quasi-species pool and to be generated *de novo*. First, the sequences of the integrase (IN) regions of the four primary isolates were determined. Table 1 shows the detailed evaluation of the R5/X4 mixture subtype B (KP-1), R5-CRF08_BC (KP-2), R5 subtype B (KP-3) and X4-CRF01_AE (KP-4) primary isolates, and the dual-tropic subtype B laboratory virus (89.6). Although some naturally occurring polymorphisms were observed within the IN regions of these isolates compared with the subtype B consensus sequence available from the Los Alamos National Laboratory HIV sequence database, we did not identify any primary resistant mutations to RAL. Three baseline viruses (KP-1, KP-4 and 89.6) were sensitive to RAL, with IC_{50} values ranging from 1.2 to 4 nM, which are comparable with those reported previously (Kobayashi *et al.*, 2008). However, KP-2 and KP-3 showed minor resistance to RAL, with IC_{50} values of 16 and 32 nM, respectively. These two isolates contained amino acid mutations at positions 72, 125 and 201 within the IN region [previously reported as L-870,810 and S-1360 resistance mutations (Hombrouck *et al.*, 2008; Rhee *et al.*, 2008), but not as RAL-resistance mutations]. KP-2 also contained a unique insertion at position 288 (NQDME) at the C-terminal end of the IN region.

In vitro selection of variants of the primary isolates and 89.6 using RAL

To induce RAL-selected HIV-1 variants *in vitro*, PM1/CCR5 cells, a T-cell line expressing high levels of CCR5, were exposed to the four primary isolates and strain 89.6. The viruses were then serially passaged in the presence of RAL. As a control, each isolate was passaged under the same conditions, but without RAL, to allow monitoring of spontaneous changes occurring in the viruses during prolonged PM1/CCR5 cell passage (the passage control). The selected viruses were initially propagated at a RAL concentration equal to each IC_{50} value. The RAL concentrations were then increased from 20 to 85 nM during the course of the selection procedure (Table 1).

Only small shifts in the IC_{50} to RAL were observed in four of the five isolates (KP-1, KP-2, KP-4 and 89.6), with fold changes in IC_{50} values of 3.4, 6.5, 16 and 9.2, respectively. KP-3 did not show resistance to RAL. IC_{50} values in all the passage controls were comparable with those of the baseline viruses (Table 1).

IN region sequences in RAL-selected variants

The full-length *IN* genes were amplified and cloned to determine the genetic basis of selection in the presence or absence of RAL. Ten to 12 clones from each sample were sequenced.

Substitutions within IN were observed at passages 30 (G189R) and 29 (T210I) in two RAL-selected isolates (KP-2 and KP-4, respectively). Neither of these has been reported as IN inhibitor-resistant mutations. No substitutions in the IN regions of KP-3 and 89.6 were found. However, A125T and V180I substitutions were observed in the KP-3 and 89.6 control variants at the last passage. No previously reported mutations were identified in the IN region of KP-1 (an R5/X4 mixture isolate) after 17 passages. However, four amino acids (K7/K111/H216/D278) were selected by RAL from the baseline quasi-species, whereas different amino acids (R7/R111/Q216/N278) were selected in the control-passage variants (Table 1).

Taken together, these findings showed that RAL-induced selection pressure causes adaptation within the IN regions of bulk primary viruses during *in vitro* passage in the target cells, and confirmed that this system can be used to analyse drug-selected variants *in vitro*.

Comparison of *env* gene sequences in RAL-selected and passage-control isolates

A highly diverse gp120 region was observed in the baseline R5/X4 mixture isolate, KP-1; however, the viral diversity of variants passaged in the presence or absence of RAL decreased significantly during *in vitro* selection (overall mean distance after RAL selection of 0.056 at baseline to 0.007 after passage 17; mean overall distance in the passage control of 0.01 after 20 passages, Table 2). Moreover, the RAL-selected and control variants utilized CCR5 to enter the target cell; neither variant used CXCR4 (Table 3).

Interestingly, the low-diversity RAL-selected variant contained a completely different Env sequence from that of the passage-control variant (Fig. 1a). Different regions spanning

Table 1. Susceptibility of HIV-1 isolates to RAL and distinct differences in IN region sequences between RAL-selected and control-passaged viruses

Isolate	Subtype	Tropism	Passage no.	Concn (nM)	RAL-selected variant*		Passage control	
					IN sequence	RAL IC_{50} (nM)	IN sequence	RAL IC_{50} (nM)
KP-1	B	Mix	0	0	*K/R7, K/R111, Q/H216, D/N278*	4	*K/R7, K/R111, Q/H216, D/N278*	4
			8	20	**K**111, **H**216, **D**278	31 (7.8)	**R**7, **R**111, **Q**216, **N**278	4.5 (1.2)
			17†	20	**K**7, **K**111, **H**216, **D**278	26 (6.5)	**R**7, **R**111, **Q**216, **N**278	0.4 (0.1)
KP-2	CRF08_BC	R5	0	0	*I201, ins289NQDME*	16	*I201, ins289NQDME*	16
			18	40	G189G/R, *I201, ins289NQDME*	32 (2)	*I201, ins289NQDME*	16 (1)
			30	85	G189R, *I201, ins289NQDME*	55 (3.4)	*I201, ins289NQDME*	25 (1.6)
KP-3	B	R5	0	0	*V72, A125*	32	*V72, A125*	32
			11	25	*V72, A125*	25 (0.78)	*V72, A125*	33 (1)
			22	27.5	*V72, A125*	37 (1.2)	*V72*, A125T	13 (0.41)
KP-4	CRF01_AE	X4	0	0	–	2.1	–	2.1
			8	40	–	33 (16)	R166R/K, D279N	4.4 (2.1)
			29	40	T210I	22 (10)	G163E, R166R/K, D279N/S	4.1 (2)
89.6	B	R5X4	0	0	–	1.2	–	1.2
			8	15	–	34 (28)	–	4.4 (3.7)
			34	20	–	11 (9.2)	V180I	1.2 (1)

*Amino acid changes in each passage variant are shown. Italicized letters represent mutations relative to the consensus subtype BC or B present in the baseline isolates. Bold letters represent amino acids selected out of the quasi-species cloud. The fold increase in RAL IC_{50} values is shown in parentheses for *in vitro*-selected variants compared with those in the baseline isolates.
†The RAL variant selected after 17 passages was compared with the control selected after 20 passages.

Table 2. Comparison of amino acid length and number of PNGs between RAL-selected and control-passage KP-1 variants

	Passage no.	Genetic diversity*	Mean ENV $_{1-474}$ length (range)†	Mean V1/V2 length (range)	Mean V3 length (range)	Mean V4 length (range)	Mean PNGs (range)
Baseline	0	0.056	472 (461–480)	69 (60–74)	34 (33–34)	30 (29–31)	24 (22–28)
RAL-selected virus	2	0.038	479 (472–480)‡	74 (71–74)‡	34 (33–34)‡	31 (29–31)‡	27 (25–28) ‡
	8	0.0070	480	74	34	31	28 (26–29)
	17	0.0070	480	74	34	31	27 (26–27)§
Passage control	2	0.045	464 (461–466)‡	64 (60–74)‡	34 (33–34)‡	29 (29–31)‡	24 (22–27)‡
	8	0.0070	463 (462–463)	62	34	29	23 (22–23)
	10	0.0080	462 (459–463)	62	34	29	23 (22–23)
	20	0.010	463	62	34	29	23 (22–23)§
P value			<0.0001‡	<0.0001‡	0.91‡	0.0048‡	0.0019‡ <0.0001§

*Overall mean distance.
†Sequence from gp120 SP to the V5 region (aa 1–474).
‡, § *P* values were calculated using the homoscedastic *t*-test between the RAL-selected and the passage-control variants indicated by the same symbols above.

the whole envelope sequence [from the signal peptide (SP) to V5] were compared in the RAL-selected and passage-control viruses. The results showed that, after only two passages, the gp120, V1/V2 and V4-loop regions within RAL-selected variants were longer than those in the control variants, and the number of putative *N*-linked glycosylation sites (PNGs) was significantly higher than that in the control-passage viruses (Table 2). This phenomenon was seen consistently in two independent experiments.

We also analysed the gp120 sequences in the other four isolates. Although the number of positional differences between the RAL-selected and passage-control variants for these four isolates was lower than that in KP-1 (between three and nine, compared with >40), there was a similar pattern of separation between the Env sequences (Fig. 1). In three of the four isolates (KP-2, KP-3 and KP-4), positional differences were observed in SP, C1 and all the variable regions of gp120 (Fig. 1b–d). In strain 89.6, differences were observed in the C2, C3 and V4 regions (Fig. 1e).

These results suggested that RAL treatment of target cells causes a decrease in viral diversification within quasi-species Env regions via a route different from that in untreated target cells.

In vitro induction of RAL-selected V3-loop library virus variants

To investigate further the effects of RAL on viral Env sequences, we used the V3-loop library virus (JR-FL-V3Lib) developed by Yusa *et al.* (2005), which carries a set of random combinations from zero to ten substitutions (27 648 possibilities) in the V3 loop (residues 305, 306, 307, 308, 309, 317, 319, 322, 323 and 326; V3 loop from Cys^{296} to Cys^{331}). The variants contained in the library were polymorphic mutations derived from 31 R5 clinical isolates (Yusa *et al.*, 2005). PM1/CCR5 cells were exposed to the JR-FL-V3Lib and serially passaged in the presence of RAL. After two passages, the V3 sequence within the RAL-selected variant was completely different from that in the passage control (Fig. 1f). This suggested that, under pressure from RAL, the infectious clone harbouring different V3 region sequence from the passage control had adapted to the target cells, despite containing the same IN sequences.

Phylogenetic analysis of the Env regions after passage with or without RAL

To confirm the temporal and spatial differences observed in each of the RAL-selected and passage-control viruses, phylogenetic analyses were conducted using complete SP–V5 sequences. The neighbour-joining phylogenetic tree showed a clear and distinct branching between RAL-selected and passage-control KP-1 viruses (Fig. 2a). We also identified a similar pattern in all the other isolates tested (Fig. 2b–e).

Table 3. Comparison of amino acid length, number of potential *N*-linked glycosylation sites, V3 sequences and co-receptor usage between anti-retroviral drug-selected and control-passaged KP-1 variants

	Passage no.	Genetic diversity*	Mean ENV_{1-474} length (range)†	Mean V1/V2 length (range)	Mean V3 length (range)	Mean V4 length (range)	Mean PNGs (range)	V3 region		Geno2 pheno (%)§
								Prevalence (%)	Sequence‡	
Baseline	0	0.056	472 (461–480)	69 (60–74)	34 (33–34)	30 (29–31)	24 (22–28)	41.9	CTRPNNNTRKGIHIGPGKFYATGAIIGDIRQAHC	41.2
								22.6	.....V.....	41.2
								16.1	....-..I.....T.R..T.RD...N..K...	1.7
								13.0	....-..I.....T.R..T.KT...N.KK...	2.9
								3.2	....-..I.....	7.4
								3.2	.....D.....	55.3
Passage control	8	0.0070	463 (462–463)	62	34	29	23 (22–23)	100.0	.....V.....	41.2
RAL-selected virus	8	0.0070	480	74	34	31	28 (26–29)	100.0	.....	41.2
3TC-selected virus	6	0.020	478 (475–480)	74	34	31 (29–31)	27 (25–28)	83.3	.....	41.2
SQV-selected virus	11	0.0040	474	71	34	31	26	100.0	.....	41.2
MVC-selected virus	7	0.0080	469 (468–469)	69	33	29	24 (23–24)	100.0	....-..I....R..T.R..T.KT...N.KK...	1.7

*Overall mean distance.

†Sequence from gp120 SP to the V5 region (aa 1–474).

‡V3 sequences of each variant are shown. Dots denote sequence identity and dashes indicate a deletion mutation.

§Prediction of viral co-receptor tropism using Geno2pheno based on a selectable 'false positive rate'.

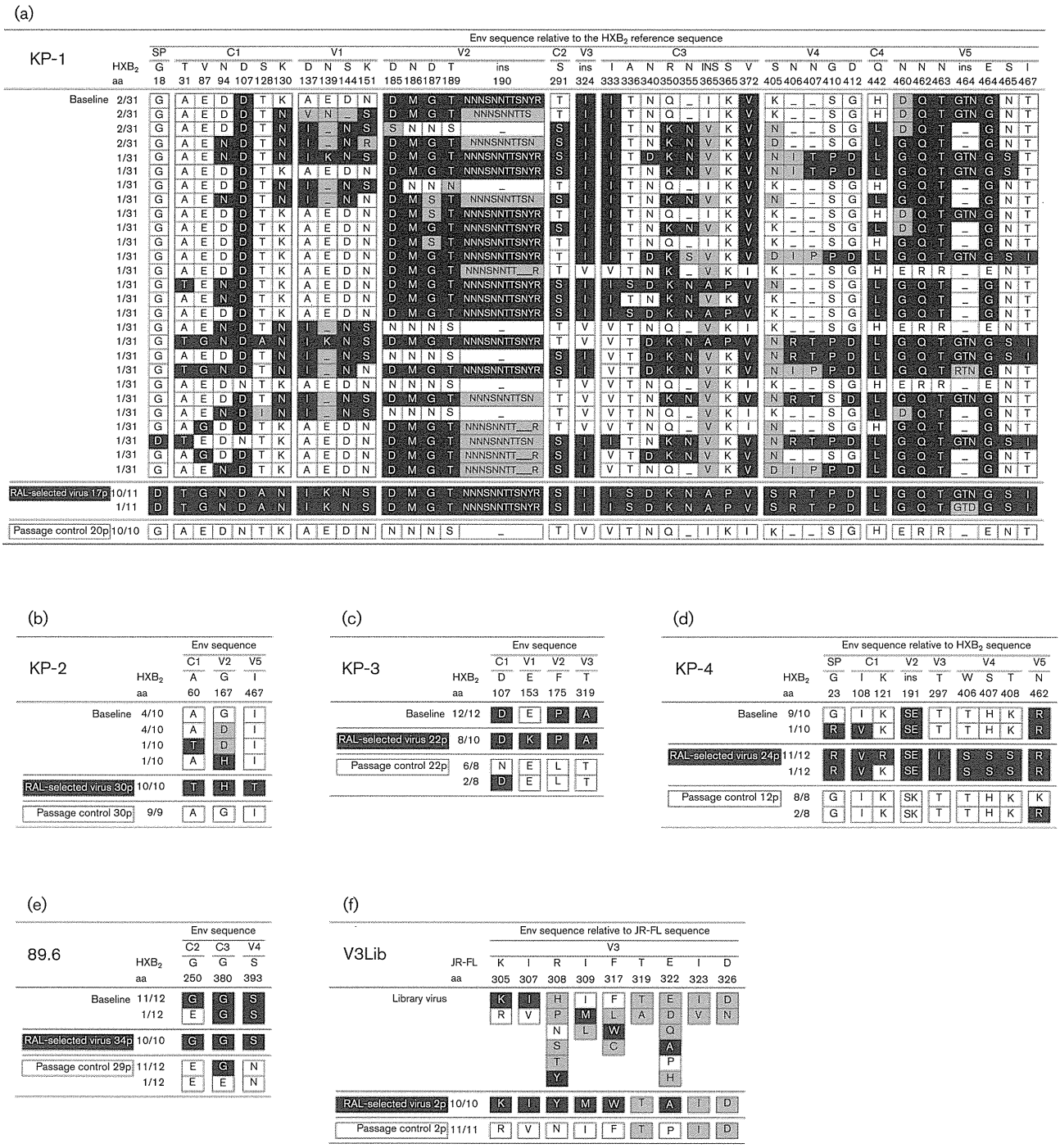

Fig. 1. Comparison of the gp120 sequences between RAL-selected and control-passaged viruses. The gp120 sequences of baseline, RAL-selected and the passage-control viruses were aligned for KP-1 (a), KP-2 (b), KP-3 (c), KP-4 (d) and strain 89.6 (e). Each amino acid in (a)–(e) is numbered relative to the HIV-1 HXB_2 reference sequence. The V3 sequences from the JR-FL-V3Lib baseline library, RAL-selected and passage-control viruses were aligned (f). Filled cells denote the most dominant amino acids observed in RAL-selected variants at the latest passage, open cells denote the most dominant amino acids observed in the passage-control variants at the latest passage and shaded cells show amino acids deleted by the end of both passages, whilst '–' indicates a deletion mutation. The number of passages is indicated, e.g. 17p for passage 17.

In vitro selection of KP-1 variants by 3TC, SQV and MVC

To determine whether other HIV drugs also changed the route of adaptation to the target cells, we attempted to select KP-1 variants using a reverse transcriptase inhibitor (3TC), a protease inhibitor (SQV) and a CCR5 inhibitor (MVC). As shown in Fig. 2(f), the pattern of clustering at distinct positions between the selected isolates and the passage-control variants was similar to that observed for the RAL-selected variants. The selected variants showed decreased diversity in the gp120 sequences; however, the length of the gp120, V1/V2 and V4 sequences increased (apart from in the MVC-selected variants). In addition, the number of PNGs within gp120 was higher than that in the control (Table 3). We also compared the V3 sequences between the passage-control and each of the drug-selected variants. The V3 sequences in all the SQV-selected variants and 83.3 % of those in the 3TC-selected variants, were comparable with those in the RAL-selected variants. This was not the case for the passage controls. Comparison of variants passaged with RAL and 3TC showed that the length of the V1/V2 and V4 regions and the number of PNGs was similar; however, these parameters were different in the SQV-selected variants (Table 3). This indicated that the time at which a drug acts (e.g. during the early or late phase of the HIV life cycle) influences the selection of Env sequences. During selection with MVC, CXCR4-tropic variants were selected from the baseline mixture after seven passages.

Taken together, these results suggested that, in treated cells, different classes of anti-HIV drugs may suppress the variability of quasi-species during *in vitro* selection via a route different from that in untreated cells.

DISCUSSION

This study evaluated the impact of anti-HIV drugs on the Env bottleneck in bulk HIV-1 primary isolates during selection *in vitro*. RAL-, 3TC- and SQV-selected variants of the unique viral isolate, KP-1, harbouring both X4 and R5 variants and with a very high level of baseline viral diversity, were used to study the final destination (genetic bottleneck) of a large variety of Env sequences. Interestingly, the phylogenetic clustering of RAL-selected KP-1 variants was completely different from that of non-drug-treated controls (Fig. 2). Our results also confirmed differences in the length of the gp120, V1/V2 and V4-loop regions and in the number of PNGs (Tables 2 and 3).

It is not clear why viruses cultured under pressure from the non-Env-directed drug RAL result in different *env* genotypes compared with those without the drug. Thus, we cloned the *IN–env* region of the proviral genome from passaged viruses and sequenced the *env* and *IN* regions on the same cloned plasmid, and compared them among the baseline and passages 1, 2, 8 and 17 of the KP-1 virus. Under low concentrations of the IN inhibitor RAL, K7 was selected for at a late passage after accumulation of the other three amino acids, K111, D278 and H216, in IN. During the sequential accumulation of these four amino acids (K111, D278, H216 and K7), the RAL-selected Env sequences at passage 17 (the Env sequences shown as filled boxes in Fig. 1) sequentially accumulated mutations in the same proviral genome (Fig. S1, available in JGV Online). However, we did not find a clone including both the RAL-selected Env at passage 17 and RAL-selected IN at passage 17 in the baseline or each passaged virus, except for in the last passage. We also examined the gp120 and IN sequences of the 3TC- and SQV-selected KP-1 variants. Compared with the RAL-selected region, the variable regions of gp120 in these selected variants were very similar to each other, except for the V1/V2 region (Fig. S2). However, the passage-control variant was very different from the drug-selected variants (Fig. 1a). Furthermore, the IN sequences were different in each passaged virus: K111/D278/H216/K7 in RAL-selected, R111/D278/Q216/R7 in 3TC-selected, K111/D278/H216/R7 in SQV-selected and R111/N278/Q216/R7 in virus without drug treatment (underlined residues indicate amino acids different from those in viruses without drug treatment). To explain these results, we believe that, under pressure from anti-HIV drugs (non-entry ARVs), the virus might show a primitive reaction to select for the Env sequence and recombine from quasi-species to gain advantage for entry and/or enhance replication in target cells. Meanwhile, IN was selected from quasi-species by a direct and/or indirect effect of RAL-induced pressure. The combination of both selective pressures may affect the selection for Env and IN during adaptation in drug-treated conditions (Figs 1a and S2). These results suggest that non-entry inhibitors, such as RAL, 3TC and SQV, might also affect cell adaptation to PM1/CCR5 cells.

Many *in vivo* studies have reported the effects of the anti-HIV drug-induced bottleneck on the *env* gene (Charpentier *et al.*, 2006; Delwart *et al.*, 1998; Ibáñez *et al.*, 2000; Kitrinos *et al.*, 2005; Nijhuis *et al.*, 1998; Nora *et al.*, 2007; Sheehy *et al.*, 1996; Zhang *et al.*, 1994). However, these studies had several limitations. Because viruses were placed under *in vivo* selective pressure using at least two anti-HIV drugs and by the host immune response, it is difficult to separate the different effects and to draw clear conclusions, particularly *in vivo*. Delwart *et al.* (1998) and Kitrinos *et al.* (2005) avoided some of these limitations by employing a heteroduplex tracking assay, although *in vivo* peculiarities still remained. Therefore, we used an *in vitro* selection system using unique bulk primary isolates established in our laboratory (Hatada *et al.*, 2010; Shibata *et al.*, 2007; Yoshimura *et al.*, 2006, 2010b) to observe the effects of the anti-retroviral drug-induced bottleneck on the *IN* and *env* genes.

This selection provides a sensitive approach for analysing virus population dynamics. The effectiveness of ARV drugs can be examined during the *in vitro* passage of a single variant or mixture of variants without being affected by many of the factors encountered *in vivo*. In addition,

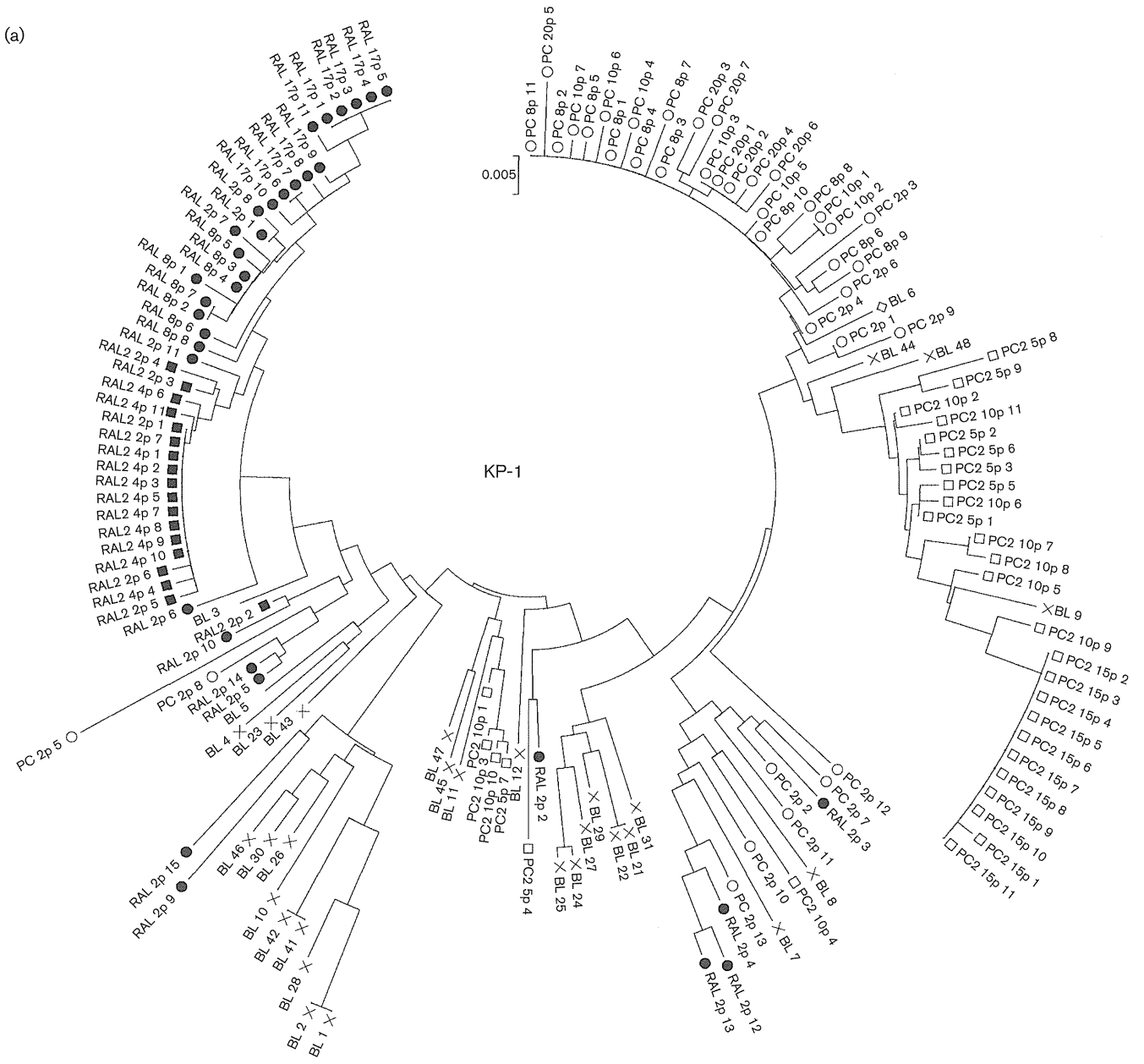

Fig. 2. Phylogenetic analyses of the Env regions from *in vitro*-passaged viruses selected with or without ARV drugs. (a–e) Phylogenetic trees were constructed using gp120 SP–V5 sequences from RAL-selected and passage-control variants of KP-1 (a), KP-2 (b), KP-3 (c), KP-4 (d) and strain 89.6 (e). An '×' represents baseline (BL) variants, and closed and open symbols represent RAL-selected (RAL) and passage-control (PC) variants, respectively. In (a), the results of the second experiment are indicated as RAL2 and PC2, respectively. (f) A phylogenetic tree was constructed using gp120 SP–V5 sequences from RAL-, 3TC-, SQV-, MVC-selected and control-passaged variants of KP-1. ○, Control variants after eight passages; ●, RAL-selected variants after eight passages; ▲, 3TC-selected variants after six passages; ◆, SQV-selected variants after 11 passages; ■, MVC-selected variants after seven passages. The trees were constructed using the neighbour-joining algorithm embedded within the MEGA software.

differences in the Env sequences between the baseline and selected variants can be compared after any number of passages. The results of the present study provide important information that will enhance our understanding of the drug-induced genetic bottleneck. This phenomenon can be examined *in vitro* using bulk primary isolates treated with or without drugs.

Recently, several new ARV drugs have been licensed for use in HIV-1-infected patients. MVC, approved in 2006, is the

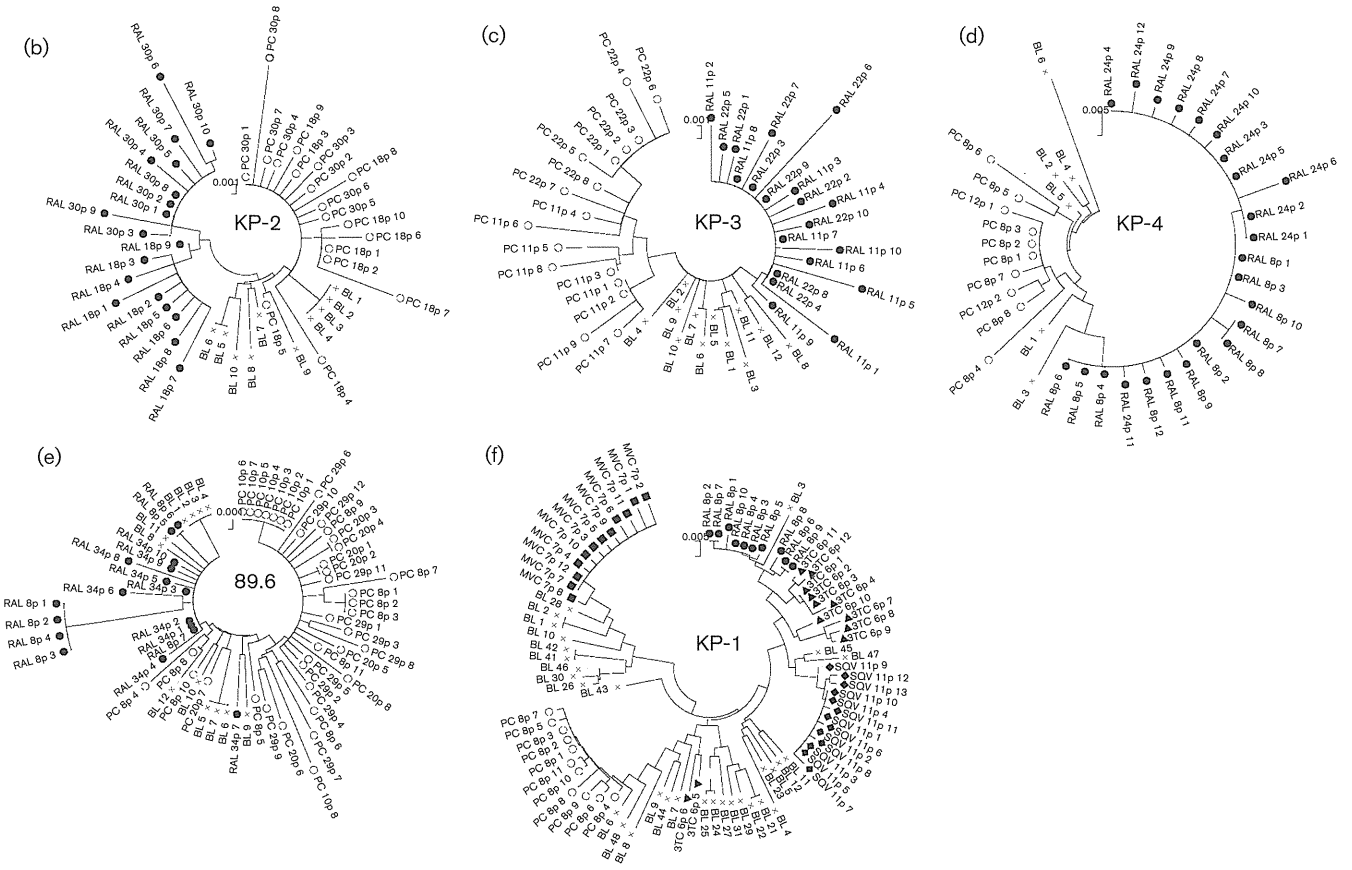

first CCR5 inhibitor (Gulick *et al.*, 2008). One important advantage associated with this drug is the absence of cross-resistance with previously available ARV compounds (Gulick *et al.*, 2008; Steigbigel *et al.*, 2008). However, as is usual with anti-HIV drugs, resistant variants with mutations in the Env, gp120 and gp41 sequences are induced both *in vivo* and *in vitro* (Anastassopoulou *et al.*, 2009; Berro *et al.*, 2009; Tilton *et al.*, 2010; Yoshimura *et al.*, 2009, 2010a). As shown in the present study, distinct Env sequences from each quasispecies might be selected by the different anti-HIV drugs (e.g. length of the V1/2 and/or V4 regions, V3 region depletion and the number of PNGs). Moreover, many of the novel anti-retroviral drugs in pre-clinical trials are viral entry inhibitors (e.g. PRO140, ibalizumab, BMS-663068 and PF-232798; Jacobson *et al.*, 2010; McNicholas *et al.*, 2010; Nettles *et al.*, 2011; Stupple *et al.*, 2011; Toma *et al.*, 2011). Therefore, it is necessary to examine whether such entry inhibitors are effective when used alongside conventional drugs.

In conclusion, we studied the genetic bottleneck in bulk primary HIV-1 isolates from untreated patients and drugs targeting the Env (and other) regions. The results showed, for the first time, the presence of drug-selected Env sequences in these isolates. Although our observations were based on a limited number of HIV-1 isolates and need to be confirmed by independent studies, we believe that they provide a new paradigm for HIV-1 evolution in the new combination ARV therapy era.

METHODS

Patients and isolates. Primary HIV-1 isolates were isolated from four drug-naïve patients in our laboratory (KP-1–4) and passaged in phytohaemagglutinin-activated PBMCs. Infected PBMCs were then co-cultured for 5 days with PM1/CCR5 cells (a kind gift from Dr Y. Maeda; Maeda *et al.*, 2008; Yusa *et al.*, 2005) and the culture supernatants were stored at −150 °C (Hatada *et al.*, 2010; Shibata *et al.*, 2007; Yoshimura *et al.*, 2006, 2010b).

After isolation of the primary viruses, we checked the sensitivity of each primary isolate to MVC. The KP-1 isolate was relatively MVC-resistant compared with KP-2 and KP-3 (54 vs 5.9 and 8.7 nM, respectively). KP-1 became MVC sensitive after eight passages in PM1/CCR5 cells [IC_{50}, 3.4 nM; Geno2pheno value (see below), 41.2 %], whilst under the pressure of MVC, KP-1 became highly resistant to MVC after eight passages (IC_{50}, >1000 nM; Geno2pheno value, 1.7 %). These results indicated that the bulk KP-1 isolate used in this study harboured primarily R5 viruses with X4- or dual-tropic viruses as a minor population.

Cells, culture conditions and reagents. PM1/CCR5 cells were maintained in RPMI 1640 (Sigma) supplemented with 10 % heat-inactivated FCS (HyClone Laboratories), 50 U penicillin ml^{-1}, 50 μg streptomycin ml^{-1} and 0.1 mg G418 (Nacalai Tesque) ml^{-1}. MVC, RAL and SQV were kindly provided by Pfizer, Merck & Co. and Roche Products, respectively. 3TC was purchased from Wako Pure Chemical Industries.

The laboratory-adapted HIV-1 strain 89.6, which was obtained through the NIH AIDS Research and Reference Reagent Program, was propagated in phytohaemagglutinin-activated PBMCs. The viral-competent library pJR-FL-V3Lib, which contains 176 bp V3–loop DNA fragments with 0–10 random combinations of amino acid substitutions, was introduced into pJR-FL, as described previously (Yusa *et al.*, 2005).

***In vitro* selection of HIV-1 variants using anti-HIV drugs.** The four primary HIV isolates (KP-1–4), strain 89.6 and JR-FL-V3Lib were treated with various concentrations of RAL and used to infect PM1/CCR5 cells to induce the production of RAL-selected HIV-1 variants, as described previously, with minor modifications (Hatada *et al.*, 2010; Shibata *et al.*, 2007; Yoshimura *et al.*, 2006, 2010b). Briefly, PM1/CCR5 cells (4×10^4 cells) were exposed to 500 $TCID_{50}$ HIV-1 isolates and cultured in the presence of RAL. Virus replication in PM1/CCR5 cells was monitored by observing the cytopathic effects. The culture supernatant was harvested on day 7 and used to infect fresh PM1/CCR5 cells for the next round of culture in the presence of increasing concentrations of RAL. When the virus began to propagate in the presence of the drug, the compound concentration was increased further. Proviral DNA was extracted from lysates of infected cells at different passages using a QIAamp DNA Blood Mini kit (Qiagen). The proviral DNAs obtained were then subjected to nucleotide sequencing. *In vitro* selection of the KP-1 isolate using SQV, 3TC and MVC was also performed using the procedure described above.

Amplification of proviral DNA and nucleotide sequencing. Proviral DNA was subjected to PCR amplification using PrimeSTAR GXL DNA polymerase and Ex-*Taq* polymerase (Takara), as described previously (Hatada *et al.*, 2010; Shibata *et al.*, 2007; Yoshimura *et al.*, 2006, 2010b). The primers used were 1B and H for the gp120 region (Hatada *et al.*, 2010; Shibata *et al.*, 2007; Yoshimura *et al.*, 2006, 2010b), IN 1F (5′-CAGACTCACAATATGCATTAGG-3′) and IN 1R (5′-CCTGTATGCAGACCCCAATATG-3′) for the *IN* region, and IN 1F and H for the *IN*–gp120 region. The first-round PCR products were used directly in a second round of PCR using primers 2B and F (Hatada *et al.*, 2010; Shibata *et al.*, 2007; Yoshimura *et al.*, 2006, 2010b) for gp120, IN 2F (5′-CTGGCATGGGTACCAGCACACAA-3′) and IN 2R (3′-CCTAGTGGGATGTGTACTTCTGAACTTA-3′) for *IN*, and IN 2F and F for *IN*–gp120. The PCR conditions used were as described above. The second-round PCR products were purified and cloned into a pGEM-T Easy Vector (Promega) or pCR-XL-TOPO Vector (Invitrogen), and the *env* and *IN* regions in both the passaged and selected viruses were sequenced using an Applied Biosystems 3500xL Genetic Analyzer and a BigDye Terminator v3.1 Cycle Sequencing kit (Applied Biosystems). Phylogenetic reconstructions were generated using the neighbour-joining method embedded in the MEGA software (http://www.megasoftware.net) (Tamura *et al.*, 2007). Overall, mean distances for viral diversity were also calculated using MEGA software. The number and location of putative PNGs were estimated using *N*-GlycoSite (http://www.hiv.lanl.gov/content/sequence/GLYCOSITE/glycosite.html) from the Los Alamos National Laboratory database.

Susceptibility assay. The sensitivity of the passaged viruses to various drugs was determined as described previously with minor modifications (Hatada *et al.*, 2010; Shibata *et al.*, 2007; Yoshimura *et al.*, 2006, 2010b). Briefly, PM1/CCR5 cells (2×10^3 cells per well) in 96-well round-bottomed plates were exposed to 100 $TCID_{50}$ of the viruses in the presence of various concentrations of drugs and incubated at 37 °C for 7 days. The IC_{50} values were then determined using a Cell Counting Kit-8 assay (Dojindo Laboratories). All assays were performed in duplicate or triplicate.

Predicting co-receptor usage by the V3 sequence. HIV-1 tropism was inferred using Geno2pheno [coreceptor] program, with a false rate positive (FPR) value of 5.0 %, which is freely available (http://coreceptor.bioinf.mpi-inf.mpg.de/index.php). This genotyping tool more accurately predicts virological responses to the CCR5 antagonist MVC in ARV-naïve patients than a reference phenotypic tropism test (Sing *et al.*, 2007).

Statistical analyses. Pairwise comparisons of the different parameters between variants in the two groups was calculated using the homoscedastic *t*-test. A P value of <0.05 was considered statistically significant.

ACKNOWLEDGEMENTS

We are grateful to Dr Yosuke Maeda for providing the PM1/CCR5 cells. We also thank Syoko Yamashita, Yoko Kawanami, Noriko Shirai and Akiko Shibata for technical assistance. This study was supported in part by the Ministry of Education, Culture, Sports, Science and Technology, Japan, by a Grant-in-Aid for Young Scientists (B-22790163); grants from the Ministry of Health, Labour and Welfare; the Program of Founding Research Centers for Emerging and Re-emerging Infectious Diseases; and the Global COE program Global Education and Research Center Aiming at the Control of AIDS.

REFERENCES

Anastassopoulou, C. G., Ketas, T. J., Klasse, P. J. & Moore, J. P. (2009). Resistance to CCR5 inhibitors caused by sequence changes in the fusion peptide of HIV-1 gp41. *Proc Natl Acad Sci U S A* **106**, 5318–5323.

Berro, R., Sanders, R. W., Lu, M., Klasse, P. J. & Moore, J. P. (2009). Two HIV-1 variants resistant to small molecule CCR5 inhibitors differ in how they use CCR5 for entry. *PLoS Pathog* **5**, e1000548.

Charpentier, C., Nora, T., Tenaillon, O., Clavel, F. & Hance, A. J. (2006). Extensive recombination among human immunodeficiency virus type 1 quasispecies makes an important contribution to viral diversity in individual patients. *J Virol* **80**, 2472–2482.

Delwart, E. L., Pan, H., Neumann, A. & Markowitz, M. (1998). Rapid, transient changes at the *env* locus of plasma human immunodeficiency virus type 1 populations during the emergence of protease inhibitor resistance. *J Virol* **72**, 2416–2421.

Eigen, M. (1993). The origin of genetic information: viruses as models. *Gene* **135**, 37–47.

Gulick, R. M., Lalezari, J., Goodrich, J., Clumeck, N., DeJesus, E., Horban, A., Nadler, J., Clotet, B., Karlsson, A. & other authors (2008). Maraviroc for previously treated patients with R5 HIV-1 infection. *N Engl J Med* **359**, 1429–1441.

Hatada, M., Yoshimura, K., Harada, S., Kawanami, Y., Shibata, J. & Matsushita, S. (2010). Human immunodeficiency virus type 1 evasion of a neutralizing anti-V3 antibody involves acquisition of a potential glycosylation site in V2. *J Gen Virol* **91**, 1335–1345.

Hombrouck, A., Voet, A., Van Remoortel, B., Desadeleer, C., De Maeyer, M., Debyser, Z. & Witvrouw, M. (2008). Mutations in human immunodeficiency virus type 1 integrase confer resistance to the naphthyridine L-870,810 and cross-resistance to the clinical trial drug GS-9137. *Antimicrob Agents Chemother* **52**, 2069–2078.

Ibáñez, A., Clotet, B. & Martínez, M. A. (2000). Human immunodeficiency virus type 1 population bottleneck during indinavir therapy causes a genetic drift in the env quasispecies. *J Gen Virol* **81**, 85–95.

Jacobson, J. M., Thompson, M. A., Lalezari, J. P., Saag, M. S., Zingman, B. S., D'Ambrosio, P., Stambler, N., Rotshteyn, Y., Marozsan, A. J. & other authors (2010). Anti-HIV-1 activity of weekly or biweekly treatment with subcutaneous PRO 140, a CCR5 monoclonal antibody. *J Infect Dis* **201**, 1481–1487.

Kitrinos, K. M., Nelson, J. A., Resch, W. & Swanstrom, R. (2005). Effect of a protease inhibitor-induced genetic bottleneck on human immunodeficiency virus type 1 *env* gene populations. *J Virol* **79**, 10627–10637.

Kobayashi, M., Nakahara, K., Seki, T., Miki, S., Kawauchi, S., Suyama, A., Wakasa-Morimoto, C., Kodama, M., Endoh, T. & Oosugi, E. (2008). Selection of diverse and clinically relevant integrase inhibitor-resistant human immunodeficiency virus type 1 mutants. *Antiviral Res* **80**, 213–222.

Maeda, Y., Yusa, K. & Harada, S. (2008). Altered sensitivity of an R5X4 HIV-1 strain 89.6 to coreceptor inhibitors by a single amino acid substitution in the V3 region of gp120. *Antiviral Res* **77**, 128–135.

McNicholas, P., Wei, Y., Whitcomb, J., Greaves, W., Black, T. A., Tremblay, C. L. & Strizki, J. M. (2010). Characterization of emergent HIV resistance in treatment-naive subjects enrolled in a vicriviroc phase 2 trial. *J Infect Dis* **201**, 1470–1480.

Nájera, R., Delgado, E., Pérez-Alvarez, L. & Thomson, M. M. (2002). Genetic recombination and its role in the development of the HIV-1 pandemic. *AIDS* **16** (Suppl. 4), S3–S16.

Nettles, R., Schurmann, D., Zhu, L., Stonier, M., Huang, S. P., Chien, C., Krystal, M., Wind-Rotolo, M., Bertz, R. & Grasela, D. (2011). Pharmacodynamics, safety, and pharmacokinetics of BMS-663068: a potentially first-in-class oral HIV attachment inhibitor. In *18th Conference on Retroviruses and Opportunistic Infections*, abstract 49. Boston, MA.

Nijhuis, M., Boucher, C. A., Schipper, P., Leitner, T., Schuurman, R. & Albert, J. (1998). Stochastic processes strongly influence HIV-1 evolution during suboptimal protease-inhibitor therapy. *Proc Natl Acad Sci U S A* **95**, 14441–14446.

Nora, T., Charpentier, C., Tenaillon, O., Hoede, C., Clavel, F. & Hance, A. J. (2007). Contribution of recombination to the evolution of human immunodeficiency viruses expressing resistance to antiretroviral treatment. *J Virol* **81**, 7620–7628.

Rhee, S.-Y., Liu, T. F., Kiuchi, M., Zioni, R., Gifford, R. J., Holmes, S. P. & Shafer, R. W. (2008). Natural variation of HIV-1 group M integrase: implications for a new class of antiretroviral inhibitors. *Retrovirology* **5**, 74.

Sheehy, N., Desselberger, U., Whitwell, H. & Ball, J. K. (1996). Concurrent evolution of regions of the envelope and polymerase genes of human immunodeficiency virus type 1 observed during zidovudine (AZT) therapy. *J Gen Virol* **77**, 1071–1081.

Shibata, J., Yoshimura, K., Honda, A., Koito, A., Murakami, T. & Matsushita, S. (2007). Impact of V2 mutations on escape from a potent neutralizing anti-V3 monoclonal antibody during in vitro selection of a primary human immunodeficiency virus type 1 isolate. *J Virol* **81**, 3757–3768.

Sing, T., Low, A. J., Beerenwinkel, N., Sander, O., Cheung, P. K., Domingues, F. S., Büch, J., Däumer, M., Kaiser, R. & other authors (2007). Predicting HIV coreceptor usage on the basis of genetic and clinical covariates. *Antivir Ther* **12**, 1097–1106.

Steigbigel, R. T., Cooper, D. A., Kumar, P. N., Eron, J. E., Schechter, M., Markowitz, M., Loutfy, M. R., Lennox, J. L., Gatell, J. M. & other authors (2008). Raltegravir with optimized background therapy for resistant HIV-1 infection. *N Engl J Med* **359**, 339–354.

Stupple, P. A., Batchelor, D. V., Corless, M., Dorr, P. K., Ellis, D., Fenwick, D. R., Galan, S. R., Jones, R. M., Mason, H. J. & other authors (2011). An imidazopiperidine series of CCR5 antagonists for the treatment of HIV: the discovery of N-(1S)-1-(3-fluorophenyl)-3-[(3-endo)-3-(5-isobutyryl-2-methyl-4,5,6,7-tetrahydro-1H-imidazo[4,5-c]pyridin-1-yl)-8-azabicyclo[3.2.1]oct-8-yl]propylacetamide (PF-232798). *J Med Chem* **54**, 67–77.

Tamura, K., Dudley, J., Nei, M. & Kumar, S. (2007). MEGA4: Molecular Evolutionary Genetics Analysis (MEGA) software version 4.0. *Mol Biol Evol* **24**, 1596–1599.

Tilton, J. C., Wilen, C. B., Didigu, C. A., Sinha, R., Harrison, J. E., Agrawal-Gamse, C., Henning, E. A., Bushman, F. D., Martin, J. N. & other authors (2010). A maraviroc-resistant HIV-1 with narrow cross-resistance to other CCR5 antagonists depends on both N-terminal and extracellular loop domains of drug-bound CCR5. *J Virol* **84**, 10863–10876.

Toma, J., Weinheimer, S. P., Stawiski, E., Whitcomb, J. M., Lewis, S. T., Petropoulos, C. J. & Huang, W. (2011). Loss of asparagine-linked glycosylation sites in variable region 5 of human immunodeficiency virus type 1 envelope is associated with resistance to CD4 antibody ibalizumab. *J Virol* **85**, 3872–3880.

Vignuzzi, M., Stone, J. K., Arnold, J. J., Cameron, C. E. & Andino, R. (2006). Quasispecies diversity determines pathogenesis through cooperative interactions in a viral population. *Nature* **439**, 344–348.

Yoshimura, K., Shibata, J., Kimura, T., Honda, A., Maeda, Y., Koito, A., Murakami, T., Mitsuya, H. & Matsushita, S. (2006). Resistance profile of a neutralizing anti-HIV monoclonal antibody, KD-247, that shows favourable synergism with anti-CCR5 inhibitors. *AIDS* **20**, 2065–2073.

Yoshimura, K., Harada, S., Hatada, M. & Matsushita, S. (2009). Mutations in V4 and C4 regions of the HIV-1 CRF08-BC envelope induced by the in vitro selection of Maraviroc Confer cross-resistance to other CCR5 inhibitors. In *16th Conference on Retroviruses and Opportunistic Infections*, p. 640. Montreal, Canada.

Yoshimura, K., Harada, S. & Matsushita, S. (2010a). Two step escape pathway of the HIV-1 subtype C primary isolate induced by the in vitro selection of Maraviroc. In *17th Conference on Retroviruses and Opportunistic Infections*, abstract 535. San Francisco, CA.

Yoshimura, K., Harada, S., Shibata, J., Hatada, M., Yamada, Y., Ochiai, C., Tamamura, H. & Matsushita, S. (2010b). Enhanced exposure of human immunodeficiency virus type 1 primary isolate neutralization epitopes through binding of CD4 mimetic compounds. *J Virol* **84**, 7558–7568.

Yusa, K., Maeda, Y., Fujioka, A., Monde, K. & Harada, S. (2005). Isolation of TAK-779-resistant HIV-1 from an R5 HIV-1 GP120 V3 loop library. *J Biol Chem* **280**, 30083–30090.

Zhang, Y. M., Dawson, S. C., Landsman, D., Lane, H. C. & Salzman, N. P. (1994). Persistence of four related human immunodeficiency virus subtypes during the course of zidovudine therapy: relationship between virion RNA and proviral DNA. *J Virol* **68**, 425–432.

JVI Journals.ASM.org

Conformational Epitope Consisting of the V3 and V4 Loops as a Target for Potent and Broad Neutralization of Simian Immunodeficiency Viruses

Takeo Kuwata,[a] Kaori Takaki,[a] Kazuhisa Yoshimura,[b] Ikumi Enomoto,[a] Fan Wu,[c] Ilnour Ourmanov,[c] Vanessa M. Hirsch,[c] Masaru Yokoyama,[d] Hironori Sato,[d] Shuzo Matsushita[a]

Center for AIDS Research, Kumamoto University, Kumamoto, Japan[a]; AIDS Research Center, National Institute of Infectious Diseases, Tokyo, Japan[b]; Laboratory of Molecular Microbiology, NIAID, NIH, Bethesda, Maryland, USA[c]; Pathogen Genomics Center, National Institute of Infectious Diseases, Tokyo, Japan[d]

Inducing neutralizing antibodies (NAb) is the key to developing a protective vaccine against human immunodeficiency virus type 1 (HIV-1). To clarify the neutralization mechanism of simian immunodeficiency virus (SIV), we analyzed NAb B404, which showed potent and broad neutralizing activity against various SIV strains. In 4 SIVsmH635FC-infected macaques, B404-like antibodies using the specific VH3 gene with a long complementarity-determining region 3 loop and λ light chain were the major NAbs in terms of the number and neutralizing potency. This biased NAb induction was observed in all 4 SIVsmH635FC-infected macaques but not in 2 macaques infected with a SIV mix, suggesting that induction of B404-like NAbs depended on the inoculated virus. Analysis using Env mutants revealed that the V3 and V4 loops were critical for B404 binding. The reactivity to the B404 epitope on trimeric, but not monomeric, Env was enhanced by CD4 ligation. The B404-resistant variant, which was induced by passages with increasing concentrations of B404, accumulated amino acid substitutions in the C2 region of gp120. Molecular dynamics simulations of the gp120 outer domains indicated that the C2 mutations could effectively alter the structural dynamics of the V3/V4 loops and their neighboring regions. These results suggest that a conformational epitope consisting of the V3 and V4 loops is the target for potent and broad neutralization of SIV. Identifying the new neutralizing epitope, as well as specifying the VH3 gene used for epitope recognition, will help to develop HIV-1 vaccines.

Neutralizing antibodies (NAb) against human immunodeficiency virus type 1 (HIV-1) protect against viral challenge in nonhuman primate models (1–5), suggesting that NAb induction may be an important key to the development of vaccines against HIV-1. The role of NAbs in prevention of infection and control of viral replication has been suggested in several studies using candidate vaccines (6–8). However, the difficulties in inducing NAbs, especially those that are broadly reactive to various HIV-1 strains, have hampered the development of such vaccines (9–11). Monoclonal antibodies (MAb) with broad neutralizing activity that were recently isolated from HIV-1-infected patients have been characterized to understand the specificities and mechanisms of broad neutralization (12–16). The epitopes of these potent and broad NAbs, such as PG9, PGT128, VRC01, and 10E8, have been determined precisely (17–19) and provide an opportunity for structure-based vaccine design to develop antibody-based vaccines for HIV-1 (11, 20–23).

Nonhuman primate models of simian immunodeficiency virus (SIV) infection are commonly used to develop vaccines against HIV-1 (6, 8, 24). Various immunogens, vectors, and regimens have been evaluated by challenge infection with SIV. Moreover, immune factors associated with prevention of infection have been explored in the SIV model. However, epitopes for potent and broad neutralization of SIV remain unclear because few MAbs that neutralize a wide range of SIV strains have been available. Recently, we isolated MAbs from a rhesus macaque infected with SIVsmH635FC, which was isolated from a rapid progressor macaque (25). Infection with SIVsmH635FC, a highly neutralization-sensitive molecular clone, resulted in a vigorous and potent antibody response in all the infected macaques together with viral mutations to escape antibody recognition (26, 27). MAb B404 bound to a conformational epitope on gp120 of various SIV strains and did not react to overlapping peptides of SIV Env. The V3 region was shown to be important by competition enzyme-linked immunosorbent assay (ELISA) with anti-V3 antibodies (25). The neutralizing activity of B404 against homologous neutralization-sensitive SIVsmH635FC, genetically divergent SIVmac316, and neutralization-resistant SIVsmE543-3 was observed.

In this study, we analyzed the epitope of B404 and the induction of B404-like NAbs in SIV-infected macaques. Analysis of more than 400 anti-Env MAbs demonstrated that B404-like NAbs with the same gene usage and specificity were mainly induced in 4 SIVsmH635FC-infected macaques. The B404 epitope was mapped to a conformational epitope consisting of the V3 and V4 loops exposed on a trimeric Env structure after CD4 binding. The identification of the new neutralizing epitope and vigorous antibody response to this epitope in SIV-infected macaques will help us to understand broad neutralization in a macaque model of SIV infection.

MATERIALS AND METHODS

Cells and viruses. PM1 (28) and PM1/CCR5 (29) cells were maintained in RPMI 1640 medium containing 10% fetal bovine serum (FBS). TZM-bl

Received 22 January 2013 Accepted 25 February 2013
Published ahead of print 6 March 2013
Address correspondence to Shuzo Matsushita, shuzo@kumamoto-u.ac.jp.

doi:10.1128/JVI.00201-13

(30–33) and 293T (34) cells were maintained in Dulbecco's modified Eagle medium containing 10% FBS. Infectious molecular clones, SIVsmE543-3 (35), SIVsmH635FC (27), SIVmac239 (36), SIVmac316 (37), SIVsmE660FL14, SIVsmH805-24w-3, and SIVsmH807-24w-4 (38) were transfected into 293T cells. After 2 days, the supernatants were filtered (0.45 μm) and stored at −80°C as virus stocks.

Construction of Fab libraries from SIV-infected macaques. The Fab library from SIVsmH635FC-infected rhesus macaque H723 was described previously (25). The Fab libraries from SIV-infected rhesus macaques H704, H709, H714, H711, and H725 (26, 27, 39) were similarly constructed using the pComb3X system according to the instructions of Barbas et al. (40). Four macaques, H723, H704, H709, and H714, were infected with SIVsmH635FC. H711 was infected with a combination of SIVsmE543-3 and SIVsmH635FC. H725 was infected with plasma samples from 2 SIVsmH445-infected macaques, H631 and H635. Rhesus macaques of Indian origin were used in this study. RNA was extracted from lymphocytes from the lymph nodes of these macaques using an RNeasy minikit (Qiagen, Hilden, Germany) and used for subsequent RT-PCR using oligo(dT)20 primer, ReverTra Ace (Toyobo, Osaka, Japan), and Platinum high-fidelity *Taq* DNA polymerase (Invitrogen, Carlsbad, CA). Two libraries, κ and λ light chains, were constructed for each macaque to examine the frequency of NAbs in each population, although only one library, containing both κ and λ light chains, was constructed for H723. Immunoglobulin (Ig) genes were inserted into pComb3X, and the ligation mix was used for transformation of XL1-Blue (Stratagene, La Jolla, CA) by electroporation. Transformed cultures were incubated in superbroth medium with 50 μg/ml carbenicillin, 10 μg/ml tetracycline, and 1.4 μg/ml kanamycin overnight at 37°C after addition of VCSM13 helper phage (Stratagene). Library phage stock was obtained from the culture medium by polyethylene glycol 8000–NaCl precipitation. Library size was determined by assessing the number of CFU after infection of XL1-Blue with a diluted phage sample.

Biopanning to obtain anti-Env antibodies. Biopanning was performed using SIV antigen (Ag), which was prepared by infection of PM1 cells with SIVsmE543-3 as previously described (25). To obtain Fab clones against Env, we selected Fab clones from the H723 library using a 96-well plate in which Env was conjugated with anti-Env Fab clones B404, B408, and H301, which recognize gp120 (conformational), gp41 cluster I and gp120 V1, respectively (25). A MaxiSoap 96-well plate (Thermo Fisher Scientific, Waltham, MA) was incubated with 100 μl of 1.25 μg/ml B404, 0.625 μg/ml B408, and 10 μg/ml H301 for 1 h at 37°C. The wells were washed with phosphate-buffered saline (PBS) containing 0.05% Tween 20 (PBS-T) and blocked with 5% skim milk (Wako Pure Chemical Industries, Osaka, Japan) in PBS (MPBS) for 1 h at 37°C. After the blocking solution was discarded, the wells were incubated with 100 μl 40-fold-diluted SIV Ag for 1 h at 37°C, washed with PBS-T, and used for panning. After incubation with 50 μl of phage library for 2 h at 37°C, the wells were washed 5 times with PBS-T, and bound phage was eluted with 50 μl 100 mM glycine (pH 2.2). Amplified phage was used for the next round of panning, and 3 or 4 rounds of panning were performed. To isolate Fab clones specific to Env, we transformed phagemid DNA into TOP10F′ *Escherichia coli* cells (Invitrogen), and supernatants from isopropyl-β-D-thiogalactopyranoside (IPTG; Wako Pure Chemical Industries)-induced cultures were screened for reactivity to SIV Env using ELISA. Fab clones were purified using a His GraviTrap column (GE Healthcare, Buckinghamshire, United Kingdom), as described previously (25).

Construction of a single-chain variable fragment (scFv) form of B404. B404 Fab was previously converted into complete rhesus IgG produced from a stable cell line carrying heavy- and light-chain plasmids pHCG-B404 and pLL-B404 (25). From these plasmids, B404 scFv was constructed using the pComb3X system (40). The heavy-chain variable region (VH) was amplified using pHCG-B404 as a template and primers HSCVH35-FL (5′-GGT GGT TCC TCT AGA TCT TCC TCC TCT GGT GGC GGT GGC TCG GGC GGT GGT GGG GAG GTG CAG CTG GTG SAG TCT GG-3′) and RhSCG404-B (5′-CCT GGC CGG CCT GGC CAC TAG TGA CCG ATG GGC CCT TGG TGG AGC C-3′). The light-chain λ variable region (VL) was amplified from pLL-B404 using primers HSCLam3 (5′-GGG CCC AGG CGG CCG AGC TCG AGC TGA CTC AGC CAC CCT CAG TGT C-3′) and RhSCJLam404 (5′-GGA AGA TCT AGA GGA ACC ACC GCC TAG GAC GGT CAG CCG GGT CCC-3′). The amplified products were combined by overlapping PCR using primers RSC-F (5′-GAG GAG GAG GAG GAG GAG GCG GGG CCC AGG CGG CCG AGC TC-3′) and RSC-B (5′-GAG GAG GAG GAG GAG GAG CCT GGC CGG CCT GGC CAC TAG TG-3′), digested with SfiI, and inserted into pComb3X in a manner similar to that of Fab construction. The resultant plasmid had the B404 VL and VH regions, which were connected with an 18-amino-acid linker, a histidine tag, and a hemagglutinin (HA) tag. This plasmid was transformed into Rosetta 2 (Merck, Darmstadt, Germany), and B404 scFv was purified from the cell pellet using a His GraviTrap column.

ELISA. ELISA was performed to detect antibodies specific to SIV Ag as previously described (25, 41). Briefly, a MaxiSoap 96-well plate was coated with PBS containing 50 ng/ml concanavalin A (Sigma, St. Louis, MO) for 1 h at 37°C, and SIV Env was conjugated by incubation with 50 μl/well 10-fold diluted SIV Ag for 1 h at 37°C. Samples were added to each well at 50 μl/well with 50 μl of MPBS, and the plate was incubated for 1 h at 37°C. When the enhancement effect of soluble CD4 (sCD4) was examined, 25 μl of sample, 25 μl of sCD4, and 50 μl MPBS were added to each well. Fabs specific to SIV Env were detected with anti-HA–peroxidase (1:1,000 dilution; 3F10, Roche Molecular Biochemicals, Mannheim, Germany) and ABTS [2,2′-azinobis(3-ethylbenzthiazolinesulfonic acid)] solution (Roche Molecular Biochemicals).

Competition ELISA was performed similarly using B404 IgG as a competitor. Ag-coated wells were incubated with 50 μl MPBS and 25 μl serial dilutions of B404 IgG for 1 h at 37°C. After incubation with 25 μl subsaturating concentrations of Fab clones, Fab clone binding was detected by anti-HA–peroxidase (1:1,000) and ABTS solution.

Analysis of neutralizing antibody titers. The neutralizing capability of Fab samples was measured as the reduction in luciferase activity after infection of TZM-bl cells with various SIV strains (6, 25). In addition to Fab samples, plasma samples from SIVsmH635FC-infected macaque H704 (26) and SIVmac239-infected macaque MM324 (42) and MAb M318T (43), which recognizes the V2 region of SIV Env, were used to examine the sensitivity of SIV variants to antibody-mediated neutralization. Briefly, 100-μl portions of serially diluted samples in duplicate were incubated with 50 μl containing 200 50% tissue culture infectious doses ($TCID_{50}$) of virus in a 96-well plate. After incubation for 1 h at 37°C, 100 μl containing 1×10^5 TZM-bl cells/ml with 37.5 μg/ml DEAE dextran was added. Infected cultures were incubated for 2 days, but cultures infected with SIVsmH635FC were incubated for 3 days. After incubation, cells were lysed with 30 μl cell lysing buffer (Promega, Madison, WI) for 15 min at room temperature (RT), and 10 μl cell lysate was transferred to a 96-well black solid plate (OptiPlates-96F; Perkin-Elmer, Boston, MA) for measurements of luminescence using a GloMax 96 microplate luminometer (Promega) and a luciferase assay system (Promega). The 50 and 90% inhibitory concentrations (IC_{50} and IC_{90}, respectively) were calculated with nonlinear regression using PRISM5 and defined as the concentration that caused 50 and 90% reductions in luciferase activity, respectively, compared to that in virus control wells after the subtraction of background.

Construction of Env mutants. The *env* gene was amplified by PCR using primers SRev-F (5′-GGT TTG GGA ATA TGC TAT GAG-3′) and SEnv-R (5′-CCT ACT AAG TCA TCA TCT T-3′) and SIVsmE543-3 plasmid as a template. The PCR product was inserted into pcDNA3.1/V5-His-TOPO vector (Invitrogen). After XbaI digestion, the plasmid was ligated with an NheI-XbaI fragment from pLP-IRES2-EGFP (Clontech Laboratories Inc., Mountain View, CA) to generate a plasmid designated RE543-EGFP that expressed both enhanced green fluorescent protein (EGFP) and Env. Mutants were constructed from RE543-EGFP using PCR mutagenesis. Deletion mutants ΔV1, ΔV2, ΔV3, and ΔV4 were created by